SECONDARY USES OF BALLUTES AFTER AEROCAPTURE

A Thesis

presented to

the Faculty of California Polytechnic State University,

San Luis Obispo

In Partial Fulfillment

of the Requirements for the Degree

Master of Science in Aerospace Engineering

By

Josiah David Shelton

August 2020

COMMITTEE MEMBERSHIP

TITLE:	Secondary Uses of Ballutes after Aerocapture
AUTHOR:	Josiah David Shelton
DATE SUBMITTED:	August 2020
COMMITTEE CHAIR:	Kira Abercromby, Ph.D. Professor of Aerospace Engineering
COMMITTEE MEMBER:	Eric Mehiel, Ph.D. Professor of Aerospace Engineering
COMMITTEE MEMBER:	Daniel Wait, M.S. Lecturer Aerospace Engineering
COMMITTEE MEMBER:	William Wolfe, Ph.D. Professor of Computer Science

ABSTRACT

Secondary Uses of Ballutes after Aerocapture

Josiah David Shelton

Aerocapture is a method for spacecraft orbital insertion that is currently being assessed for use in interplanetary missions. This method would use a low periapsis hyperbolic entry orbit to induce drag allowing the spacecraft to slow down without the use of a propulsion system. This is accomplished by using a ballute (balloon parachute), which is released after the appropriate change in velocity necessary to achieve the desired planetary orbit. Once released, the ballute could deploy a secondary mission vehicle. A MATLAB simulation was run to understand the environment a secondary payload would undergo, such as heating and deceleration, as well as to study the buoyancy due to the ballute. The stability of the spacecraft during entry is also discussed.

The results showed that if the ballute can survive the aerocapture maneuver then it will be able to survive entry with a secondary payload. The deceleration from the separation of the primary and secondary payload will be large but it can be overcome. The stability of the vehicle is dependent on the location of the center of gravity. Buoyancy at Mars has little effect due to the low density of the atmosphere; at higher density atmospheres buoyancy does play a role in the payload descent. Results of the analysis show that a successful landing of a ballute with a secondary payload is possible.

ACKNOWLEDGMENTS

First and foremost, I would like to express my gratitude to my thesis advisor, Dr. Kira Abercromby, for her dedication to excellence and constructive support. Her patient guidance steered me through the process of writing a thesis that would clearly share the results of the study.

I would also like to thank Dr. Eric Mehiel, Daniel Wait, and Dr. William Wolfe; I am grateful for their assistance and willingness to serve on my thesis committee. Their input was invaluable to the completion of this project.

To my family, thank you all of your constant encouragement and support, without which this whole study would not have been possible, and to my fiancée Melissa, thank you for always being there for me and listening to me, encouraging me and always being excited to support me as I completed each milestone.

TABLE OF CONTENTS

LIST OF TABLES

LIST OF FIGURES

LIST OF TERMS

$Area$ = area in the ram direction, m^2

B = buoyancy force, newtons

C_D = drag coefficent

D = drag force, newtons

L_0 = total length of the ballute and payload system, m

L_c = position of the cg from the front, m

R_c = minor radius of torus, m

T = temperature, K

Q = heat flux, W/cm

V = ballute volume, m^3

a = acceleration m/s^2

d_1 = major diameter of torus, m

d_2 = minor diameter of inflated torus, m

k = thermal conductivity, W/m-K

m = mass of the spacecraft, kg

$\dot{q}$ = heat transfer rate, W/cm-s

r = position, m

t = time, sec

v = velocity, m/s

β = ballistic coefficient, kg/m^2

σ = Stefan-Boltzmann Constant, $W/m^2\text{-}K^4$

ε = emissivity

ρ = density, kg/m^3

μ = gravitational constant for Mars, m^3/s^2

1. Introduction

1.1 Problem Statement

When a spacecraft arrives at another planet it usually begins a propulsive burn to achieve orbit insertion at the planet. This is expensive due to the large amount of fuel needed. In order to gain more available mass, Brown and Richardson; Hall and Le; and Miller *et al.* demonstrated that aerocapture could be used to get into orbit around another planet [1,7,11]. These studies used a ballute as the method of aerocapture. Once the spacecraft had decelerated to the appropriate velocity for planetary orbit the ballute would be released and discarded [1,7,11].

Rather than discarding the ballute, reusing it could double the mission effectiveness. By using the ballute as a delivery system there is the possibility that is could be used to land on the surface. Since it is so expensive to get a mission to another planet this would help many smaller secondary payloads become reality.

Entry, descent, and landing are risky parts of any mission since the landing spacecraft must endure extreme heating and deceleration. If the ballute system is not weighted correctly it can become unstable and be destroyed. After all of that there is still the question of whether or not the ballute would be buoyant enough to keep the secondary payload suspended in the atmosphere. This work attempts to answer these questions.

1.2 Purpose of the Study

This study will show how a ballute can be used to land a spacecraft on a planet's surface. To demonstrate this there are several problems that must be addressed. Understanding how a ballute reacts during aerocapture is one of those problems; this would allow the difference between the aerocapture and the entry to be defined. This information will show how the ballute does not ned to change for entry.

This will require simulating both the aerocapture and the entry of the system. From the simulation both the heating and the deceleration can be calculated showing what environment the ballute system will experience. During entry the stability of the spacecraft must be calculated to guarantee that it will not undergo any unexpected perturbations that could destroy the spacecraft. Additionally, the buoyancy of the ballute must be calculated. This will show if, and how high, the ballute floats and thus whether or not a parachute would be required. This study will not design a mission but will combine existing information and studies to answer whether or not a ballute could deliver a secondary payload.

For this thesis, MATLAB was used to simulate the entry, descent, and landing of the payload, including the analysis of the heating and deceleration, and the study of buoyancy due to the ballute. Verification of the simulation was done by running aerocapture trajectories previously studied and comparing the results.

1.3 Structure of the Paper

This work begins by giving a review of how an aerocapture maneuver is executed in (Chatper 2), including a review of previous aerocapture studies and how those results relate to this work. In Chapter 3, the simulation method is discussed showing the equations used in the MATLAB simulation. Also shown in this chapter is the verification of the code, the assumptions used throughout this work, and the initial values for a Martian mission. The stability of the system is discussed in Chapter 4. Comparison of aerocapture and entry at Mars is shown in Chapter 5. Using the results found from the previous chapter, entry is simulated at Titan and Venus in Chapter 6. Buoyancy for all discussed mission destinations is in Chapter 7. Conclusions and future work needed are in Chapter 8.

All images, unless otherwise cited, were generated by the author in MATLAB 2011a or Microsoft Paint.

2. Ballute Literature Review

2.1 Ballutes and Aerocapture

The concept of aerocapture is not new. The idea to slow a spacecraft down using the atmosphere of the target planet has been around for many years and using a ballute is one of the ways to accomplish it. The word ballute is a portmanteau of the words “balloon” and “parachute.” Ballutes were first designed by the Goodyear Aerospace Corporation as a planetary entry parachute [3]. They were tested by dropping ballutes via helicopter and testing the deployment mortar in vacuum chambers [3]. Mortars are tubes holding a small explosive charge that propels large parachutes or ballutes out of the tube and into the airstream. Testing them in a vacuum chamber showed how well the ballutes mortar system could deploy the ballute at the low atmospheric pressure the ballute was designed for. One other test included ballute deployment during supersonic flight at 3.15 Mach [3,4]. Real world applications of this design includes decelerators for high speed bomb drops and as a part of the Gemini crew escape parachutes [5,6].

For aerocapture, the idea is to inflate the ballute behind a spacecraft, increasing the surface area, and thus the drag, of the spacecraft as it enters the atmosphere of the target planet. Aerocapture has a major advantage over propulsive capture, in that while the propulsion system is very costly in terms of mass, the mass of the ballute is minimal in comparison. Since the propulsive

mass would not be needed, it would allow for larger scientific payloads to be used on the mission.

One good example of a previously flown mission with a high mass fraction would be the Magellan spacecraft, which had the solid propellant making up 59% of its mass [4]. Being able to reduce the fuel mass would at the very least reduce the cost if not allow for a wider range of experiments to take place. Another example is a proposed Venus sample return mission that had a propellant mass fraction of 78%, whereas using a ballute reduced the mass necessary so that the mass fraction of the ballute system was only 30% [4]. Such a major mass reduction is appealing.

Deciding what materials to use to construct the ballute out of is important. The ballute material must be able to withstand the temperatures of the maneuver, be durable enough to survive the mission and properly deploy without an issue, and must obviously be qualified as space rated. Previous research has studied thin film materials for successful ballutes and two such materials have been identified [1,2]. Both meet the qualifications of being able to withstand the heat of an aerocapture maneuver, as well as being durable and lightweight space rated materials. The first material is the polymer based Polyboxoxazole (PBO) and Kapton is the other material option [4,5,9]. However Kapton seems to be slightly more popular due to its lower cost, higher availability, and the fact that it has flight heritage all while having similar characteristics to PBO [5].

A ballute is a low ballistic coefficient system. For aerocapture a large ballute would be inflated, with the larger surface area provided by the ballute a higher

periapsis can be used and would thus lower both the dynamic pressure and the heat flux [1]. The ballute is a ballistic option with no active control system. Once the spacecraft reaches the appropriate velocity for the intended capture orbit, the ballute would be released and the spacecraft would continue on to make a periapsis raising burn.

Figure 1 shows how an aerocapture maneuver would work. The spacecraft enters on a hyperbolic trajectory and passes through the atmosphere where the atmospheric drag slows down the spacecraft. After the initial aerocapture pass through the atmosphere, a burn would commence at periapsis to raise the orbit. Then if necessary a burn at apoapsis would complete the maneuver and normal orbit maneuvers could commence.

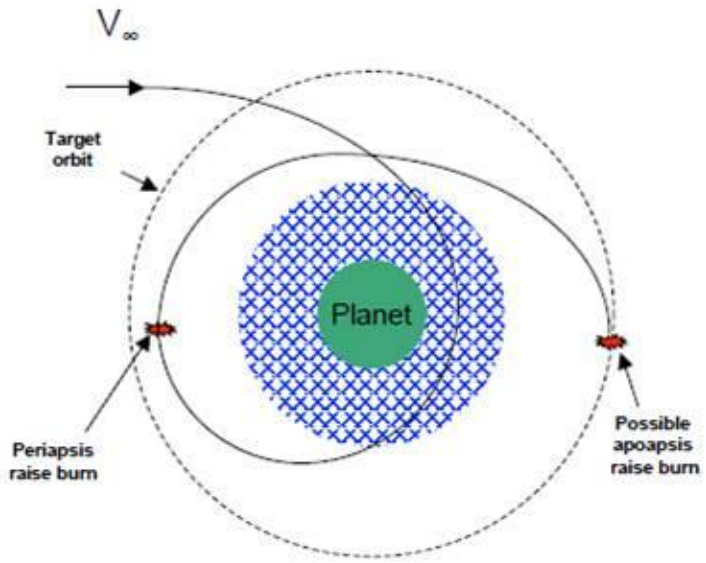

Figure 1. Diagram of aerocapture profile [2]

2.2 Ballute Configuration

One study examined the shape of the ballute and how stable it would be during entry [2]. There are two main categories of configurations for using a ballute as seen in Fig. 2. The first is a clamped configuration, where the ballute acts as an extended aeroshell with a thin film material acting as a membrane that stretches out to the toroid, giving the ballute structure. A toroid is a thick ring and with a hole in the middle-it resembles a doughnut. The second configuration, shown on the top right of Fig. 2, removes the membrane and is known as a trailing ballute. This configuration also makes use of the toroid design style and is attached to the spacecraft using cables. There are several ways the ballutes could be configured within each main category, as shown in Fig. 2, and one additional option for the trailing ballute is using a sphere instead of the toroid.

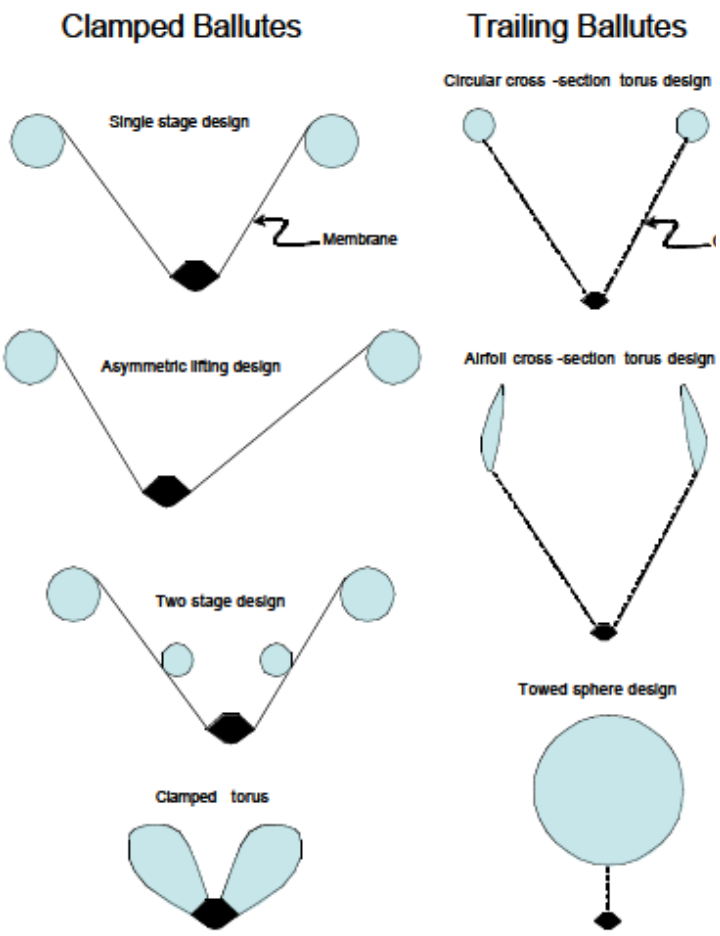

Figure 2. Ballute designs [2]

However the sphere option, bottom right in Fig. 2, is not the optimum shape for ease and stability. Since the ballute is behind the spacecraft, it is in the turbulent flow of the wake, which creates an unsteady flow around the ballute which can be seen in the pseudoschlieren image in Fig. 3 taken from a computational fluid dynamics (CFD) analysis[2]. Large scale flow instabilities could cause instability and reorientation of the system[2]. The system instabilities could be solved by increasing the towing distance[2], however, the best option is to change the shape of the ballute which not only fixes the stability problem but will also requires less gas for inflation. The toroid can be towed at a more reasonable distance and

since it has a hole in the center, the wake of the spacecraft can pass through without creating an unsteady flow regime. Pseudoschlieren images showing these responses at mach 10 are shown in Fig. 3 and Fig. 4.

After the stability and geometry of the ballute has been dealt with, the simulations of the aerocapture trajectories begin.

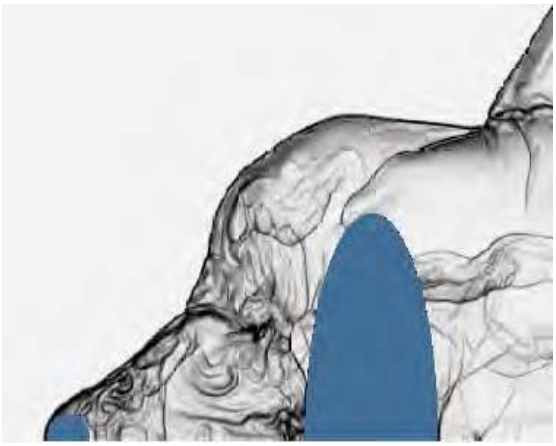

Figure 3. Unsteady flow over an elliptical ballute at Mach 10 [2]

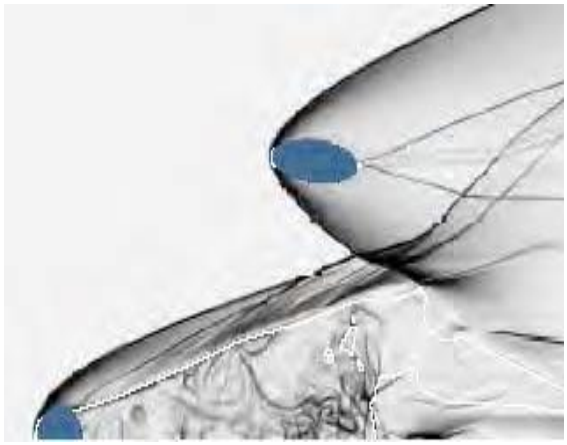

Figure 4. Steady flow around a torodial ballute at Mach 10 [2]

2.3 Aerocapture Entry Trajectory Simulation

There are several targets that are commonly evaluated for possible ballute aerocapture, and they are Mars, Titan, and Neptune. Because of the interest in ballute aerocapture, several studies have been done to analyze possible trajectories. These studies used several different methods to simulate the aerocapture. Some used a pre-built aerocapture tool such as HyperPASS^{TM}, Langley Aerothermodynamic Upwind Relaxation Algorithm (LAURA), or a Direct Simulation Monte Carlo (DSMC) analysis tool [1,11]. LAURA is a proprietary program of NASA's used to study hypersonic flow [11]. Hall and Le used MATLAB

to model a 2-D, non-lifting trajectory using a constant drag coefficient and density profiles from literature [7].

Using a torodial trailing ballute, Miller *et al.* studied the possible trajectories for aerocapture at Mars and Titan [11]. In their report they detail the full analysis which included perturbations, heating, and spacecraft configurations [11]. They created a database of several ballute sizes, all of which had a radius ratio (R/r) of 5:1 [11]. This ratio is composed of the radius of the toroid (R) and the radius of the circle that makes up the revolved surface (r). For the Titan scenario the trajectory was initiated at 1000 km altitude with a velocity of 6.5 km/s and an entry angle of 39° [11]. The 6.5 km/s velocity is typical for a low impulse trajectory with a single Venus flyby [8,11]. This trajectory was accomplished using a ballistic coefficient of 0.4 kg/m^2 [11]. The Martian entry altitude was set to 200 km with and entry speed of 5.5 km/s and an entry angle of 29° [11]. Velocities of 5.5 km/s are representative of a direct Earth to Mars trajectory [11]. Several other parameters from these trajectories are listed in table 1. Table 2 shows the results of a Monte Carlo simulation that was performed on the trajectory for Titan. This simulation took into account the perturbations on the atmosphere, the data from accelerometers, entry angle, and ballistic coefficient.

Table 1. Comparison of Mars and Titan aerocapture trajectories [2]

Characteristic	Mars	Titan
Ballute β, kg/m^2	0.8	0.4
$\beta_{\text{spacecraft}}/\beta_{\text{ballute}}$	140	145
V_{entry}, km/s	5–6	6–8
Pass duration, s	1100	3600
Velocity decrement, km/s	2.0	4.8
Peak deceleration, g	2.5	4.3
Peak heat rate, W/cm^2	2	0.9
Peak heat rate, Pa	28	46

Table 2. Monte Carlo results of Titan aerocapture [2]

Characteristic	Value
Number of failed[a] cases	0
Min. circularization ΔV	125 m/s
Max circularization ΔV	376 m/s
Mean circularization ΔV	186 m/s
Mean + 3σ circularization ΔV	285 m/s
Mean heat rate	1.9 W/cm^2
Mean + 3σ heat rate	2.1 W/cm^2

From their simulations they concluded that the Martian trajectory had a max heat flux of 2 W/cm^2 and a max deceleration of 2.5 g's[8]. While for Titan the max heat flux was 0.9 W/cm^2 and the peak deceleration was 4.3 g's [8]. This shows how an aerocapture maneuver may be designed and carried out. The studies also provide a baseline to compare results against, Verifying how accurate a simulation is as well as giving some understanding of what the magnitude of the entry conditions would be.

Lyons and Johnson studied highly eccentric aerocapture scenarios with an apoapsis of 430,000 km at Neptune [13]. They assumed a 500 kg spacecraft with three ballute sizes of 750 m^2, 1477 m^2, and 3000 m^2 [13]. They had seven values for the entry velocity that ranged from 22.4 to 27.2 km/s [13]. Using these values they obtained the heat transfer of the ballute to determine what the best trajectory and configuration would be. The results showed that a large ballute with a low entry angle would be the best for minimizing heating (Fig 5). Heating is the main difficulty for most aerocaptures since the g-load of the spacecraft stays small, below 5 g.

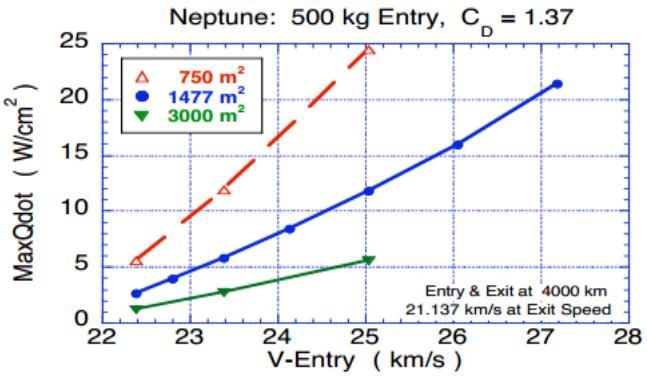

Figure 5. Maximum heat transfer versus entry speed [13]

2.4 Atmospheric Density

The challenge of aerocapture is determined by the atmospheric density of each planet. However some of the planets share similar characteristics in terms of the density profile. Mars, Venus, and Earth have similar profiles while still having different overall densities, with Mars having the lowest atmospheric density and Venus having the greatest. In comparison to Neptune and Titan who have larger atmospheres and thus a higher over all density. Figure 6 also shows the density needed for both aerocapture as well as aerobraking. This allows the altitudes for the maneuvers at each planet to be determined.

This work mentions aerocapture at each of the planets listed except for Earth. Currently there are no studies of ballute aerocapture at Earth, although it could be useful for a return mission from another planet.

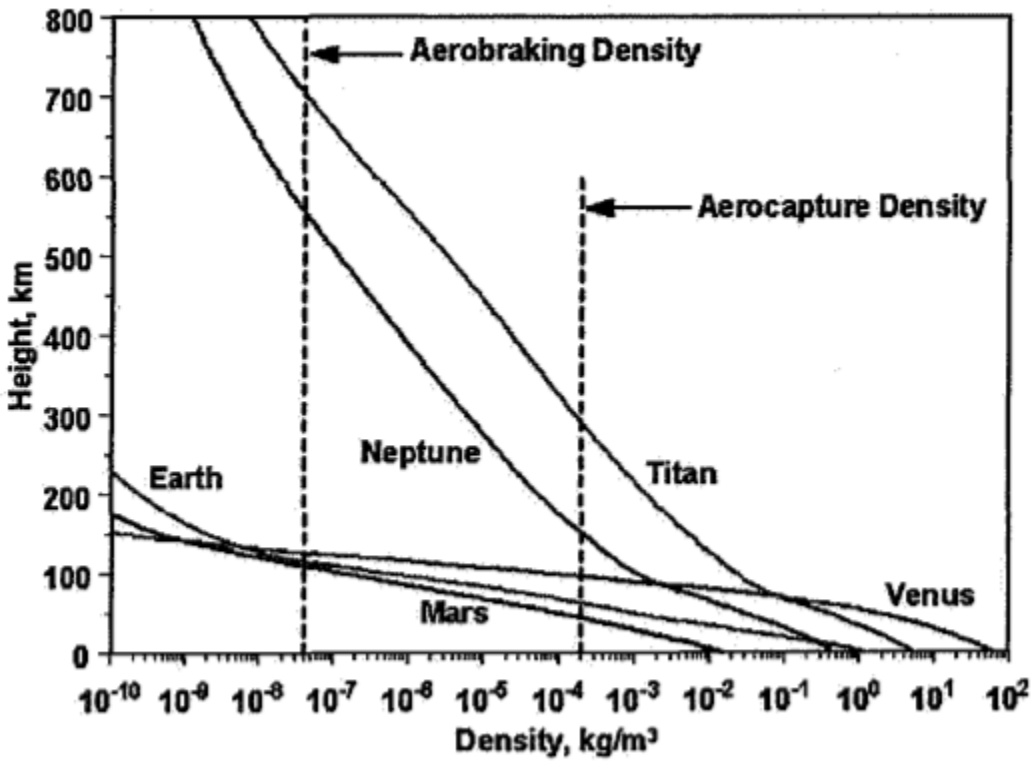

Figure 6. Comparison of typical profiles of atmospheric density for Venus, Earth, Mars, and other planets. Typical altitudes and densities for aerocapture and aerobraking are indicated [22].

2.5 Trajectory Control

Currently an aerocapture event by means of a ballute is a ballistic event with the only active control being when to release the ballute. The design of a ballute depends on a high drag ratio between the ballute and the spacecraft of about 100:1[1]. This is to allow the spacecraft to experience little to no drag once the ballute is released from the spacecraft. One method of trajectory control is using predictor-corrector algorithms. These algorithms have been developed to calculate the precise ballute release timing needed to achieve the necessary capture delta-V [8]. One algorithm that was studied performed with a one hundred percent successful capture rate throughout a Monte Carlo simulation [8]. A

histogram of the result is shown in Fig. 7 with the initial parameters for the aerocapture shown in table 3 [8].

Another possible method of trajectory control is using lift modulation to adjust how the ballute reacts in the flow. This would allow for active control measures to be used which would mean a higher accuracy of insertion into the capture orbits. Lift modulation is accomplished by attaching small actuators to the lines of the parachute [1]. This allows for the lines to be adjusted during flight changing the shape of the parachute and allowing the payload to be steered [1].

Table 3. Characteristic values for trailing and clamped ballute for aerocapture at Titan for 1000kg spacecraft [8]

Parameter	Trailing	Clamped
Torus radius, r_t	17.27 m	12.1 m
Torus cross sectional radius, r	3.45 m	1.73 m
Aspect ratio, AR = r_t / r	5	7
Ballute diameter, D	41.44 m	27.66 m
Half cone angle, q	42 deg	70 deg
Ballute attach radius, s	0 m	1.5 m
Spacecraft protruding height, h	N/A	0.5 m
Ballute aerodynamic reference area, A	748 m^2	600.8 m^2
Ballute drag coefficient, free molecular limit	2.19	2.10
Ballute drag coefficient, hypersonic	1.25	1.489
Hypersonic ballistic coefficient (1000 kg entry mass)	1.07 kg/m^2	1.12 kg/m^2

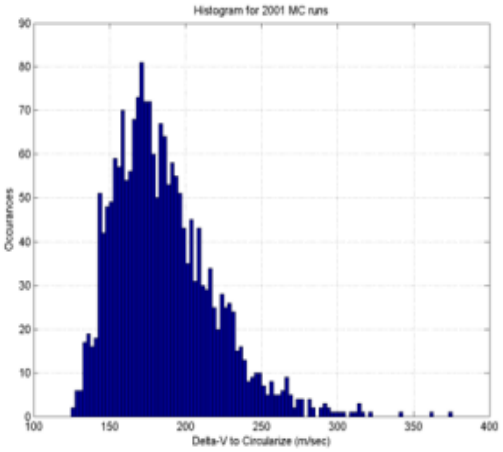

Figure 7. Circulization delta-v from Monte Carlo [8]

2.6 Real World Testing and Development

While there are no current real world ballutes under development, NASA is working to develop Hypersonic Inflatable Aerodynamic Decelerators (HIAD) [17, 18]. These will be inflatable heat shields attached to the front of the space craft. The current design uses Kevlar rings stacked together to form the structure while a thermal blanket composed of layers of heat resistant materials cover the front

to act as the thermal protection system [20]. Figure 8 shows the structural rings in the foreground as well as a completed design in the background.

Figure 8. Kevlar rings (foreground) make up the structure of the IRVE-3 [20] (background)

This completed prototype is known as IRVE-3 from the Inflatable Reentry Vehicle Experiment and was launched from a Black Brant sounding rocket to successfully splashdown in the Atlantic where it was recovered [19]. During reentry it reached Mach 10 and underwent a max temperature of 1000 °F and 20 g's acceleration [19]. This gives a glimpse as to what the real world design of a ballute might be.

2.7 Stability Theory

To ensure the accuracy of the simulation, the stability of the vehicle after separation must be checked to ensure mission completion. Park studied this and showed that in low density atmospheres the ballute is stable as long as the location of the center of gravity (cg) is in the front 43.75% of the spacecraft [12].

Anything above the 43.75% would cause the angle of attack of the ballute to rapidly rise and begin tumbling [12]. However, looking at the results of the study, Fig. 9, the stability with the cg at 43.75% was just barely acceptable. To ensure that the ballute is stable it would be best to place the cg at a position that is in the front 30% of the spacecraft. Figure 9 shows the results of the study using a ratio of the location of the cg from the front of the spacecraft (L_c) divided by the length of the spacecraft and attached ballute (L_0). This means that any study or design of a ballute system needs to pay attention to the location of the cg and at the very least keep it within the front 43% of the spacecraft.

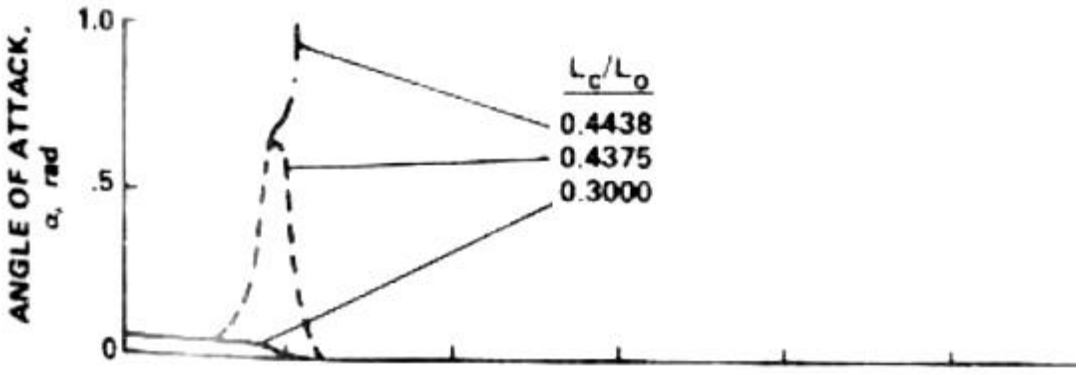

Figure 9. Variation in angle of attack for three different cg locations (L_c/L_0 values) [12]

2.8 Dual-Use Ballutes

A study, authored by Medlock *et al.*, also delved into the possibility of using a ballute to deliver a secondary payload. The study used Vinh's analytic aerocapture solution to derive the equations that would provide the maximum heating and deceleration of the system as well as the capture trajectory [21]. A similar method was used to observe the secondary payload. This approach was

used to simulate aerocapture and secondary payload release at Mars and Titan[21].

The results of the equations are compared with the ballistic coefficient of the ballute and spacecraft system [21]. The ballistic coefficient is a ratio of the mass, drag coefficient, and the cross-sectional are of the ballute and spacecraft system. When determining the peak heating rate and deceleration both the entry speed and the ballutes cross-sectional area were varied [21]. The initial values for the orbiter and the Ballute/Lander can be found in Table 4, while the entry conditions and constants used for Mars and Titan are in Table 5.

Table 4. Vehicle parameters for dual-use ballute simulations at Mars and Titan [21]

Parameter	Orbiter	Ballute/Lander
m	400 kg	100 kg
C_D	1.37	1.37
A	2 m^2	500–3000 m^2
C_B	$m/(C_dA)$	0.730–0.122 kg/m^2

Table 5. Entry conditions and atmospheric constants at Mars and Titan [21]

Condition	Mars	Titan
Reference Density, kg,m^2	$4.73e^{-10}$	$7.52e^{-10}$
Entry/Exit Altitude, km	150	1025
Inertial Entry speeds, km/s	5.75-11	6.5-10

By running the analysis to find the maximum stagnation point heating rate and the maximum deceleration using a varying entry speed and ballute size resulted in the graphs below. Figure 10 shows the maximum stagnation point heating rate on the ballute, and Fig. 11 shows the maximum deceleration on the ballute.

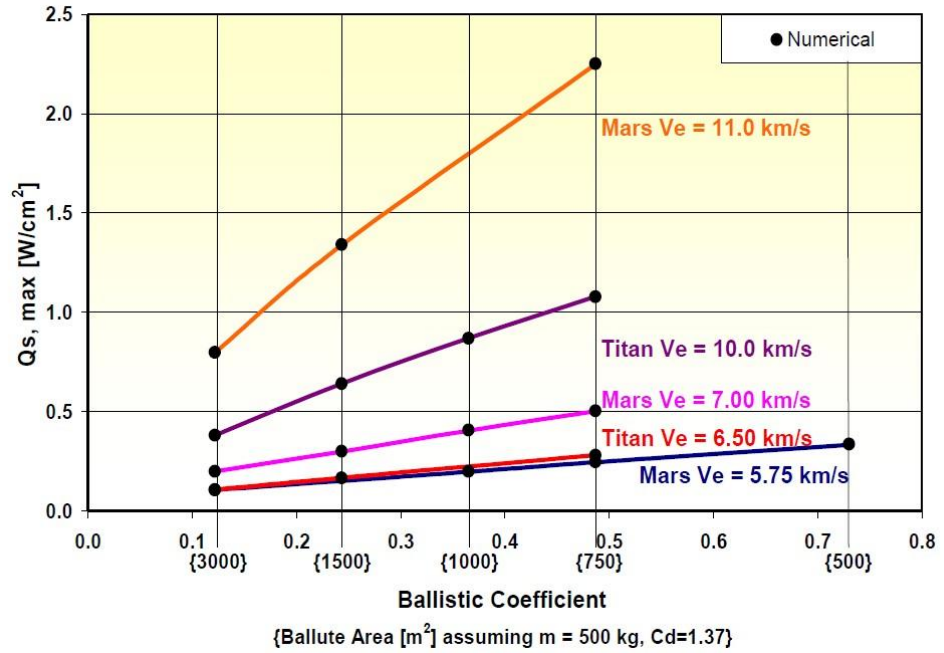

Figure 10. Maximum stagnation point heating rate (on ballute) vs. ballistic coefficient [21].

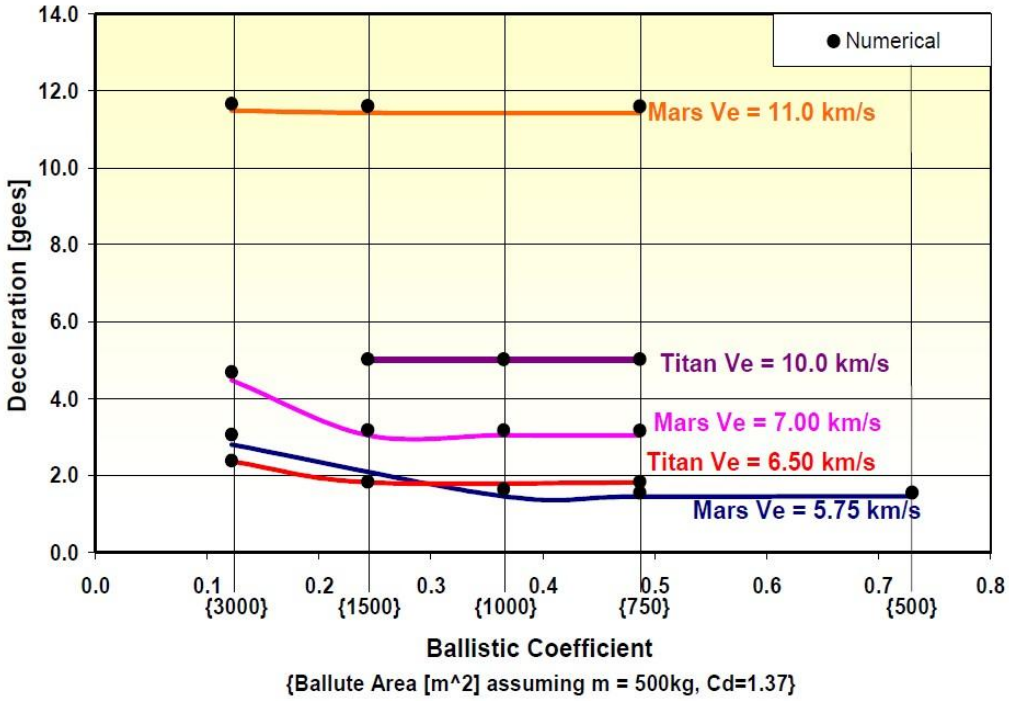

Figure 11. Maximum deceleration vs. ballistic coefficient [21].

Using a stagnation point heating limit of 5 W/cm^2 Medlock *et al.* concluded that the ballute sizes studied would work for the aerocapture maneuver and the delivery of the secondary payload [21]. They also observed that a ballute with a larger cross-sectional area would decrease the heating rate [21]. Observing the maximum deceleration showed that while the larger ballute would lower the maximum heating rate it would raise the maximum deceleration [21]. The study concludes by determining that a dual-use ballute mission is possible at Mars and Titan.

The study by Medlock *et al.* differs from this work in a few ways, which include the approach to simulating the aerocapture, and both the missions and the parameters chosen to simulate. As well as the fact that this work studies both the buoyancy effect of the ballute on the secondary payload and the stability of the spacecraft. While the conclusions put forth by Medlock *et al.* are similar to those put forth by this work Medlock *et al.* goes into more scrutiny of the derivation of the equations than the results of the simulation.

3. Procedure

3.1 Assumptions

For this study, to provide the necessary evidence in an efficient manner some assumptions had to be made to simplify the process. One such assumption is that the vehicle is stable so that the simulation does not have to take into account the rotational axes. With this assumption the cross-sectional area is constant and does not change during the entire descent. For simplicity it is also assumed that the drag coefficient is constant, which is the standard for initial studies such as this one [1,2,7,11].

It is also assumed that the heat and temperature is only due to the aerocapture maneuver. This means that heat flux and temperatures does not take into account the atmospheric temperature or the temperature of the spacecraft.

For this simulation wind was not a factor taken into consideration since it mainly affects the downrange distance and landing location. Another effect wind may have on the vehicle during descent is whipping, where the wind will cause the ballute and the payload to whip back and forth. However, since the assumption is that this is a stable payload, and since the solution to whipping requires careful design and a completely separate simulation of the ballute and the payload during the descent, this effect falls outside the scope of this study. Under these assumptions, the simulation becomes two-dimensional because the only perturbations are perpendicular to the cross-sectional area of the vehicle.

This simulation will be able to provide accurate results proving how a secondary payload is possible. It will also emphasize the challenges faced in

having a secondary payload. While it is accurate enough for a proof of concept study, it will not be precise enough to design a mission.

3.1 Analysis

MATLAB was used to code a two dimensional, non-lifting trajectory with constant drag coefficients and non-rotating atmosphere using the following equations. These equations govern the motion of the vehicle throughout the mission from space to the surface. Several equations were necessary to ensure that all effects of acceleration are accounted for in the atmosphere and above it, including the orbit equation, the drag equation, and the equation for buoyancy.

$$\vec{\boldsymbol{a}} = -\mu \frac{\vec{r}}{r^3} \tag{1}$$

$$D = \frac{1}{2}\rho v^2 C_D A \tag{2}$$

$$B = \rho V g \tag{3}$$

Where ρ is the atmospheric density, v is velocity, C_D is the drag coefficient, and A is the area in the ram direction. The drag coefficient for a Mars mission was 1.7 and is considered to be constant [1,2,7,11]. In the buoyancy equation, eq. 3, V is the volume of the ballute while g is the gravitational acceleration of the planet. For the buoyancy and drag equations, the acceleration due to the force was found by dividing the equations by the mass of the vehicle. The area used in the drag equation is the cross-sectional, or effective, area of the vehicle facing the flow. The above equations will be used to obtain the components necessary to solve the differential equations for the velocity and the position of the spacecraft. For a

two dimensional trajectory the equations for the velocity and position vectors are shown below.

$$v = dx + dy \tag{4}$$

$$r = x + y \tag{5}$$

Next the first equations were combined to obtain the vertical and horizontal components necessary to solve the differential equations. The sine and cosine of the entry angle, gamma, are used on the drag equation to get the drag for the x and y vectors.

$$\frac{d^2y}{dt^2} = -\mu\frac{y}{r^3} - \frac{1}{2m}\rho(dy)^2 C_D A \sin(\gamma) - \frac{\rho V g}{m} \tag{6}$$

$$\frac{d^2x}{dt^2} = -\mu\frac{x}{r^3} - \frac{1}{2m}\rho(dx)^2 C_D A \cos(\gamma) \tag{7}$$

Due to the fact that buoyancy only affects the vertical force, the buoyancy equation is only needed to be solved for in the y, or vertical, direction. The equations were solved in a Mars Centered Inertial coordinate frame. This is where the coordinate frame is centered on Mars with the z-axis is along the pole, the x-axis is on the intersection of the equatorial plane and the prime meridian, and y-axis is perpendicular to the plane created by the x and z. Since it is an inertial frame it does not rotate nor does it have any velocity or acceleration. Once the spacecraft has passed the Karman line, which is the boundary between space and the planet's atmosphere, the orbital equation is replaced with gravitational acceleration and the equations become as follows:

$$\frac{d^2y}{dt^2} = -g + \frac{1}{2m}\rho(dy)^2 C_D A \sin(\gamma) - \frac{\rho V g}{m} \quad (8)$$

$$\frac{d^2x}{dt^2} = -\frac{1}{2m}\rho(dx)^2 C_D A \cos(\gamma) \quad (9)$$

In these equations the density and position vary, however the mass, drag area, and coefficient of drag are constant. The numerical solutions for the equations of motion were used to determine the stagnation point heating rate, the heat flux, and the temperature.

$$\dot{q} = kv^3\sqrt{\frac{\rho}{R_c}} \quad (10)$$

The variable k in equation 10 is the coefficient of atmospheric chemistry, which is equal to 1.9207e-4 W/m-K for Mars [9]. Also R_c stands for the radius of curvature, or half of the minor diameter of the ballute, d_1; both of which are in meters. The heat flux was found by integrating the heating rate with time as shown in eq. 11. Temperature is found using the heat flux, Stefan-Boltzmann constant, and the material emissivity in eq. 12.

$$Q = \dot{q} * t \quad (11)$$

$$T = \sqrt[4]{Q\ \sigma\ \varepsilon} \quad (12)$$

Both the temperature and the heat flux are only relative to the heat added by the aerocapture maneuver. The heat due to the system is assumed to have a minimal impact.

To obtain the necessary density for the equations at the correct altitude, the density data was interpolated from the Committee on Space Research's (COSPAR) Mars Reference Atmosphere which is shown in Fig. 12 [10].

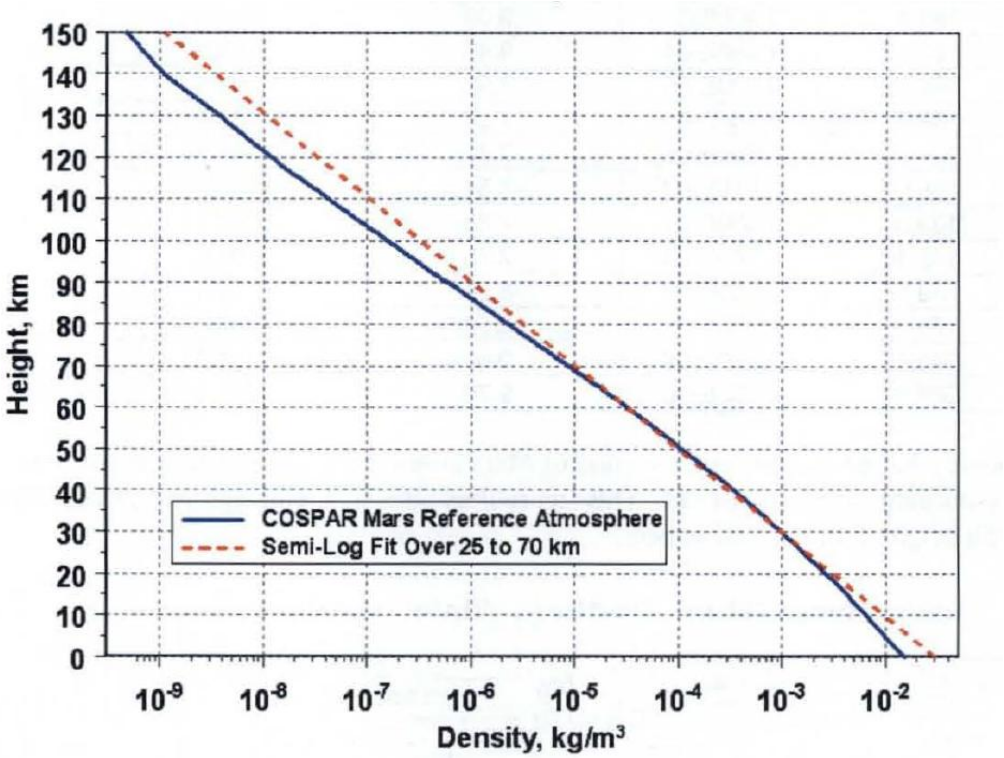

Figure 12. COSPAR Mars Reference Atmosphere density profile, compared with a semi-log best fit from 25 to 70 km [10]

Obtaining the volume of the ballute for the buoyancy and the cross-sectional area for the drag was achieved by using the following equations that use the major diameter, d_1, and minor diameter, d_2, of the ballute. The values of the diameters were obtained from the design elements found in the study the mission was based off of [7,11].

$$V = 2\pi^2 \frac{d_1}{2} \frac{d_2^2}{4} \tag{13}$$

$$A = \frac{\pi(d_1 - d_2)^2}{4} \tag{14}$$

To simulate the entry of the ballute, the equations of motion were programmed into a function that was then analyzed by the ODE45 function in MATLAB. After

the differential equation is solved, the heating equations, which are outside of the ODE, can then be solved using the results.

To ensure that the separation of the ballute and the payload occurred at the correct time, a function was setup so that after the vehicle slows down to 3700 km/s the separation will occur. Other aerocapture studies have used the 3700 km/s threshold as the separation point [7, 11]. This is due to the fact that it is close to the speed needed for an apoareion altitude of 600 km ensuring that the separation point is relatively close to the planned release point for the mission.

3.2 Code Verification

Verifying this code was merely a matter of inputting the parameters for an aerocapture mission and running the mission looking at the payload instead of the ballute. By comparing the results of the simulation to the results of the study it can be determined whether or not the simulation results are accurate. The initial inputs for the spacecraft are listed in Table 6. Miller showed a heat transfer of 2 W/cm^2 where as the verification code results showed a 2.1 W/cm^2 [11]. Deceleration was 2.5 g for Miller while the entry code resulted in 2.4 g, where g is the standard unit of one earth gravity or 9.8 m/s^2 [11]. Also the time for the vehicle to transit through the atmosphere was 200 seconds for both simulations [11]. Table 7 shows both the results of the study as well as the code results. With the results of the simulation matching quite well with the results from the Miller's study, the code is suitable for use in this study.

Table 6. Initial values code verification

Entry Angle (deg)	9
Entry Velocity (km/s)	5.5
Mass Spacecraft (kg)	400
Mass Ballute (kg)	25
Drag Coefficient, C_D	1.7
Entry Altitude (km)	200
Ballutes cross-sectional area (m^2)	300
Spacecrafts cross-sectional area (m^2)	2
Emissivity (ε)	.9

The differences in the values can be attributed to the fact that Miller *et al*. used Langley Aerothermodynamic Upwind Relaxation Algorithm (LAURA) to simulate the areocapture [11]. LAURA uses the Navier-Stokes equations to simulate the entry as well as using Direct Simulation Monte Carlo (DSMC) techniques and a DSMC Analysis Code to refine the results [11]. These options and other extra perturbations are outside the scope of this study. While not studying these perturbations and using the assumptions addressed above does have an impact, comparing the results in Table 7 shows that the impact to the findings of this study will be negligible. The results shown in Table 7 represent the peak values for heat flux and g-loading as these are the results the authors presented.

Table 7. Results from verifying the code

	Miller's Results	Verification Results
Deceleration	2.5 g	2.4 g
Heat Transfer	2 W/cm^2	2.1 W/cm^2
Time In Atmosphere	200 sec	200 sec

3.3 Initial Values

The values that were used to simulate the entry of the secondary payload at Mars and are based on values that were used in the previous aerocapture studies [7,11]. However the total system mass is now made up of both the spacecraft's mass and the combined mass of the ballute and secondary payload. The entry angle γ denotes the angle at which the spacecraft enters the atmosphere. This is taken from a range of angles running from shallow to steep. Shallow angles require the vehicle to pass through most of the atmosphere before being released, while steeper angles would require the ballute to be released at an earlier time. The mass of the secondary payload was chosen to ensure that the ballute and the vehicle would be stable upon entry in a low density atmosphere, and is based on the ballute system mass [7, 11]. These initial values are presented in Table 8, while Fig. 13 shows how some of the physical characteristics of the ballute are defined, where d_1 is the major diameter of the torus and d_2 is the minor diameter. The entire length of the spacecraft and ballute defined as L_0, all measurements in meters. The dimensions of the ballute are taken from the previous studies [7,11].

Table 8. Initial values for the ballute system

Entry Angle (deg)	7-8.2
Entry Velocity (km/s)	5-6
Mass Spacecraft (kg)	400
Mass Payload+Ballute (kg)	100
Drag Coefficient, C_D	1.7
Entry Altitude (km)	140
Ballutes cross-sectional area (m^2)	300
Spacecrafts cross-sectional area (m^2)	2
Emissivity (ε)	.9

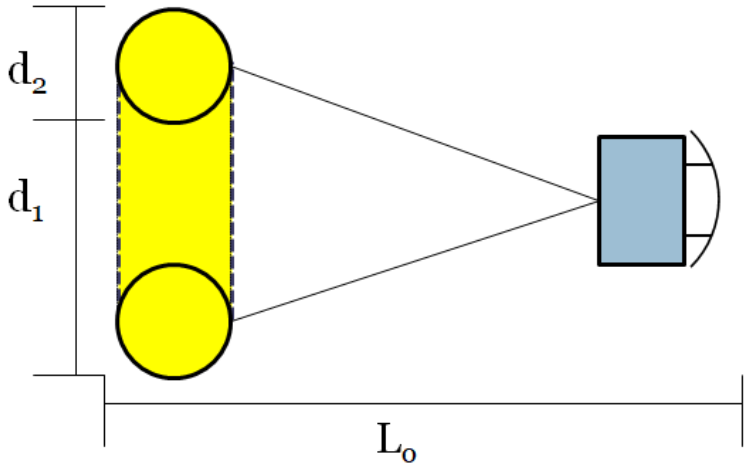

Figure 13. The spacecraft and the ballute's defining physical characteristics

4. Stability

4.1 Stability

To ensure the stability of the ballute the center of gravity must be in the front 43.75% of the payload. However since 43.75% is merely the last point before instability it is better to use a more conservative placement of 30%. Determining the cg position requires knowing both the length of the spacecraft (L_0) and the mass of the payload. This was done by assuming an initial length of 10 m. Using that length, a graph was created to show what the cg position is for a number of different masses, Fig. 14.

From this, by comparing the minimum location requirement of 43.75%, which is represented by the vertical black line, with the results it was discovered that the minimum mass for stability is 34 kg, which is represented by the red line. However, to ensure the stability, and placing the cg at a more stable position of about 30%, a 75 kg mass was chosen and is depicted on the graph with a green line. With a ballute system mass of 25 kg, the total mass of the secondary payload became 100 kg.

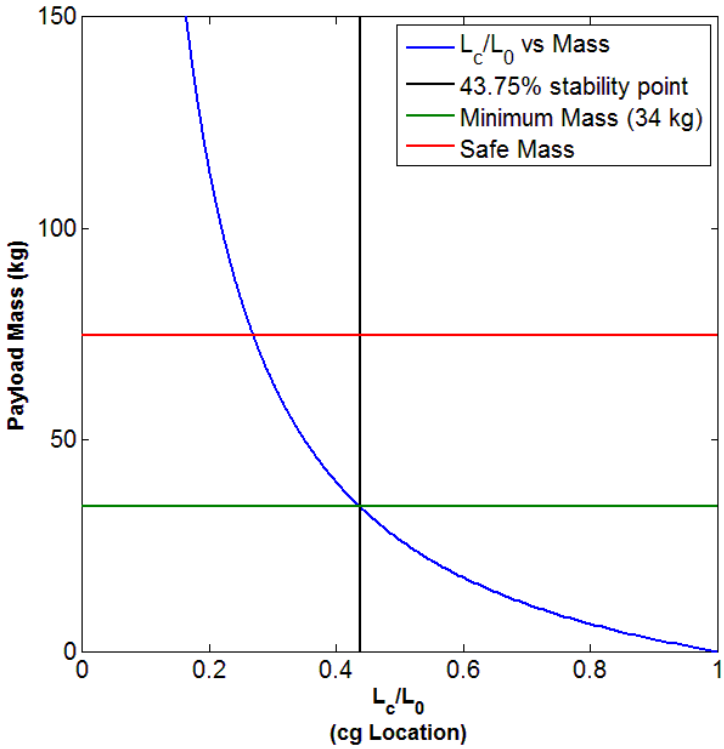

Figure 14. Stability based on the location of the cg

However, to ensure that the length of the vehicle was at the optimum, the minimum lengths for a number of different masses were charted using a brute force solution as seen in Fig. 15. This graph shows an exponential increase for the minimum vehicle length at lower payload masses. Heavier payloads are stable with a length of 10m. While a shorter length may be acceptable it is better to keep the ballute at a distance and thus away from the turbulence created by the spacecraft and the payload. This means that a vehicle length of 10m will ensure the stability of the system during entry.

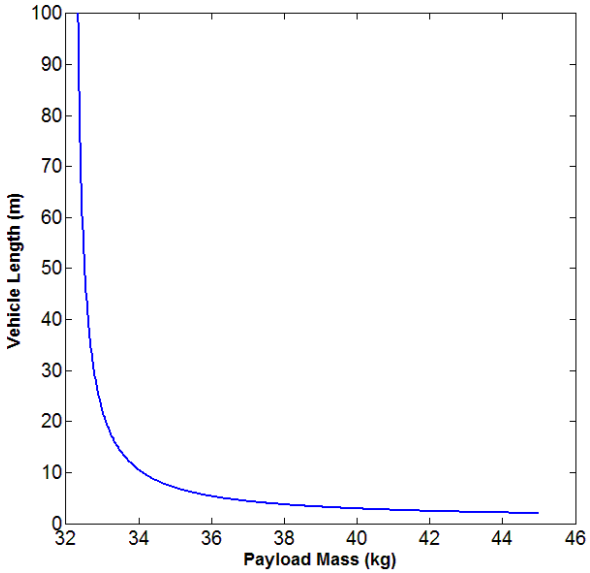

Figure 15. The trend of the minimum stable mass compared to the length of the system

5. Aerocapture and Entry at Mars

5.1 Aerocapture

To truly understand what must be done to land a secondary payload on the surface using a ballute it must be understood how the entry environment is different from that of a normal aerocapture mission. Therefore the ballute's entry is simulated using the same code that is used to simulate aerocapture. With a second payload the ballute would, upon separation, continue into the atmosphere and land on the surface while at the same time the main payload continues on to the target orbit, as shown in Fig. 16.

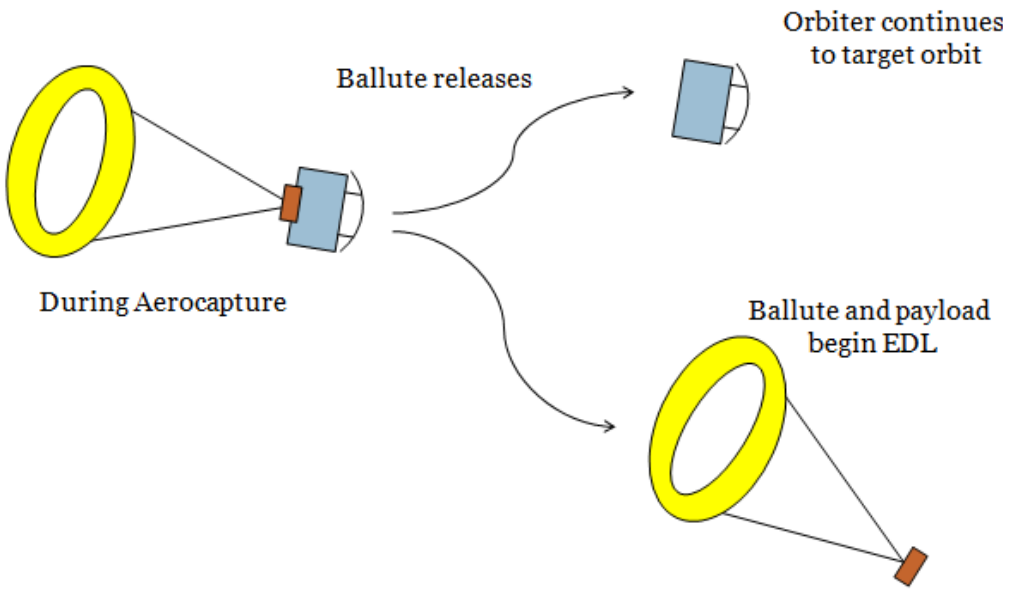

Figure 16. Showing the separation of the ballute with the second payload

To obtain the nominal entry case without a second payload, an initial entry angle of 7.6° and velocity of 5.5 km/s was used, which is the nominal case for the mission that Hall and Le used in their study *Aerocapture Trajectories for Spacecraft with Large, Towed Ballutes* [7]. The heat reached a temperature of 774° K and a heat flux of 2.2 W/cm^2 and the acceleration for this case peaked at 2.9 g's as shown in Fig. 17. These events happened at 85 and 96 seconds respectively with a starting altitude of 150 km. The temperature can be seen to drop very low. This is due to the fact that the simulation is only looking at the heating due to the entry and is not taking into account the atmospheric temperature.

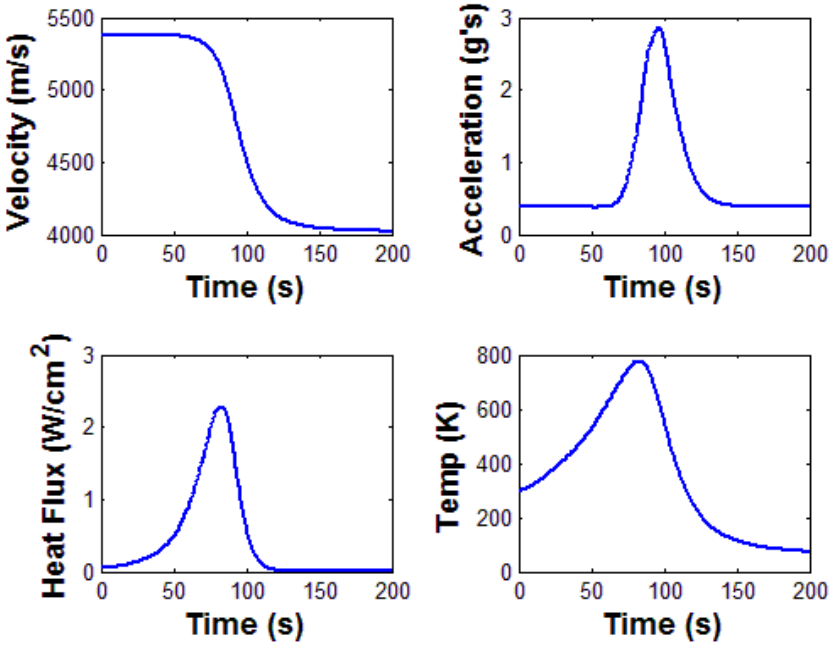

Figure 17. Graphing the velocity, acceleration, heat flux, and temperature versus time

It is important to note that these results were obtained using the assumptions of a stable space craft simulated in a two dimensional Mars Centered Inertial coordinate frame.

5.2 Entry

The nominal entry case used an entry angle of 7.6° and an entry velocity of 5.5 km/s. This case is based off of Hall and Le's study that resulted in what they considered ideal entry limits for an aerocapture maneuver [7]. When simulating this and focusing on the secondary payload it resulted in maximum values of 10 g's of deceleration, a heat flux of 2.2 W/cm^2, and a temperature of 812° K. Figure 18 shows how these variables change during the entry. At 88 seconds, separation occurs, and there is a corresponding change in the acceleration and heat flux. This is where the g-forces spike due to the separation. The heat flux, and thus the temperature, shows the separation happening after the peak.

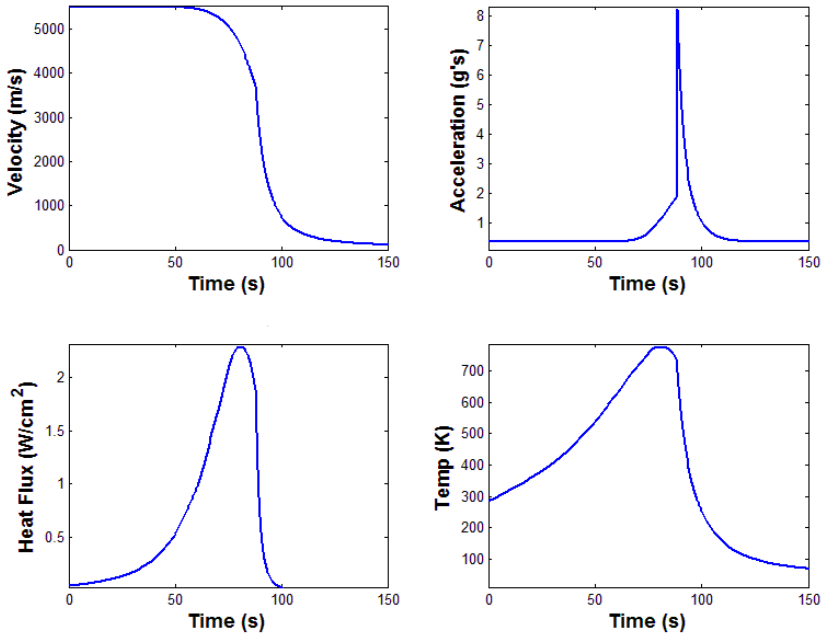

Figure 18. Time vs. velocity (upper left), acceleration (upper right), heat flux (lower left), and temperature (lower right)

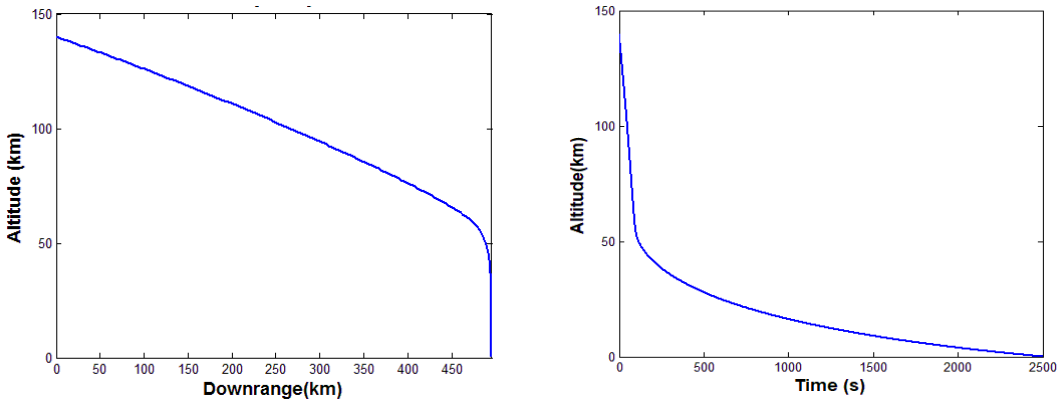

Figure 19. The trajectory of ballute and payload (L) and the altitude vs. time (R)

Figure 19 shows how the ballute system does eventually reach the surface of Mars. However taking into consideration that the drag coefficient was assumed to be constant means that it did not do so at the speed and time shown in the figure. The drag coefficient is reliant on the systems speed and atmospheric density. Since both the speed and density change drastically in the lower

atmosphere the drag coefficient should change as well. While this does affect the final velocity and time that the ballute would reach the surface it does not affect the buoyancy of the ballute, which is more connected to the volume of the ballute.

By assuming that the ring-like toroid has a similar drag coefficient as that of a cylinder at subsonic speeds, the toroid would have a drag coefficient of 1.2. Taking that into consideration an approximate landing velocity can be found. After 33 minutes the secondary payload reaches the surface with a velocity of 8.9 m/s. This means that the landing would cause 0.91 g's of force. Since this is smaller than the g-loading from entry this is a survivable landing.

The nominal case is taken from what was considered an ideal range of both the entry velocity and the entry angle. To understand what the ballute and secondary payload go through upon entry, and what the limiting factors of a secondary payload are, the simulation was run again using the minimum and maximum velocities and entry angles of the ideal range, as shown in Table 9. These entry values and ranges match with values used in several different studies of Martian aerocapture [7,11]. Running these values through the simulation obtains the extremes that may be encountered by the vehicle upon entry for a range of entry velocities and angles that were considered to be the ideal range for the mission[4].

Table 9. Ranges for the entry velocity and angle

Variable	Limits
Entry Angle, γ (deg)	7-8.2
Entry Velocity (km/s)	5-6

The results of these edge cases are presented in Fig. 20. The trajectory with the maximum heat flux and temperature had a velocity of 6km/s with an entry angle of 8.2°. The higher g-force due to separation came from the shallower 7° entry angle, but the same 6km/s velocity. As the graph shows, while the velocity does affect the deceleration and heat flux, the angle has a more drastic affect on the secondary payload. Table 10 shows the maximum values on the ballute from the simulations of the edge cases.

The results also show how the angle and speed affect the time until separation. The faster and steeper trajectories separate sooner, since they reach the high density areas quickly and slow down more rapidly. In contrast, the shallow and slower trajectories take more time, since they do not encounter the high density areas as quickly. Since the time until separation is really only a marker of when the spacecraft has decelerated enough to reach its intended orbit, the results show how quick the maneuver really is.

Table 10. Maximum values from the edge cases

Variables	Max Values
Acceleration (g's)	10
Heat Flux (W/cm^2)	2.9
Temperature (K)	812

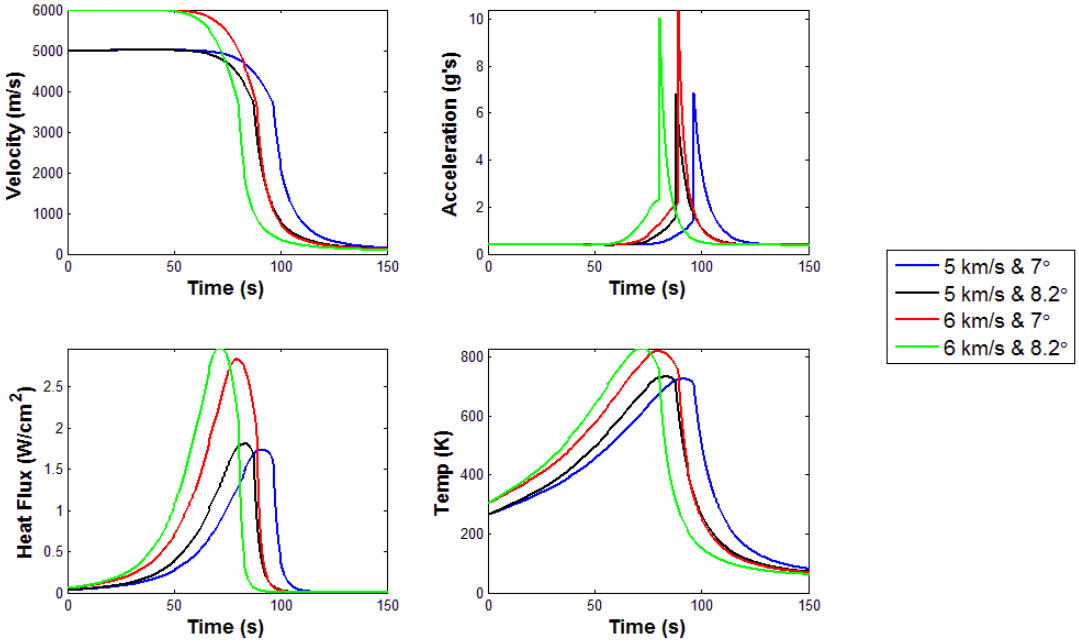

Figure 20. Edge case results for angles from 7°-8.2° and velocities from 5-6km/s

While using the given numbers to define the trajectory shows what happens according to the proposed mission, this does not mean that those values will always be used or that they will be what the secondary payload actually experiences. To determine the trends based upon the entry angles and velocities, the limits should be widened to raise the extremes. To do this the ranges of both the entry velocity and entry angle were doubled. Where the original entry angle limits had a range of 1.2° this was doubled to 2.4° and the

entry velocity range was doubled from 1 km/s to 2 km/s. The new limits are shown below in Table 11. Once the new limits were found the simulation was run again. By examining the results of a more extreme entry case it could be understood how flexible the theory is and designing for a harsher environment creates a more robust system. This simulation resulted in the trajectories shown in Fig. 21 and the maximum values in Table 12.

Table 11. Values of the entry angle and velocity

Variable	Limits
Entry Angle, γ (deg)	6.4-8.8
Entry Velocity (km/s)	4.5-6.5

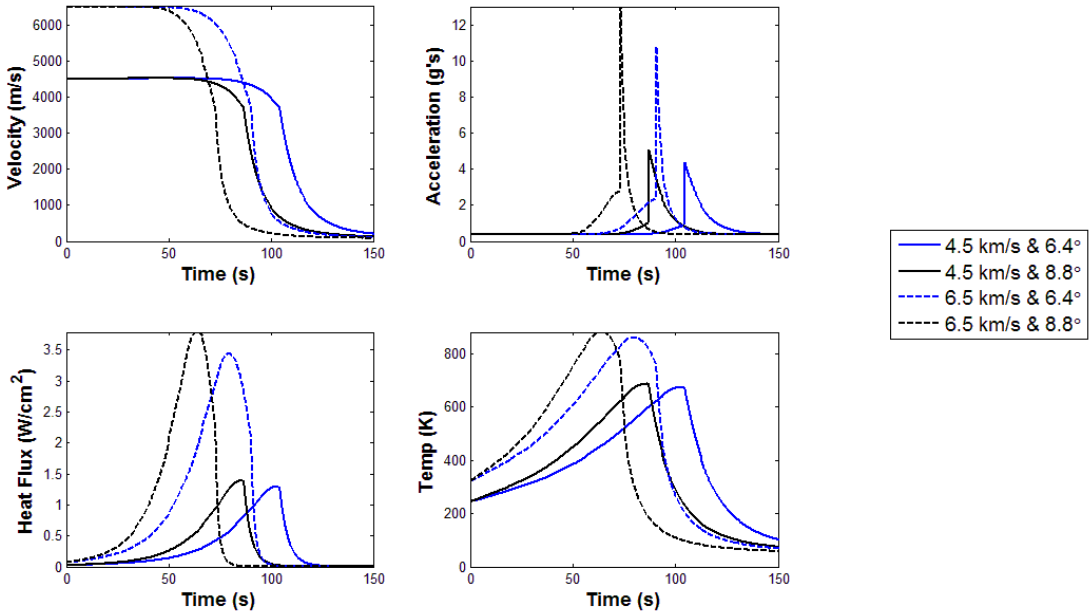

Figure 21. Extreme case results for angles from 6.4°-8.8° and velocities from 4.5-6.5 km/s

Table 12. Maximum values for the extreme double range case

Variables	Max Values
Acceleration (g's)	13
Heat Flux (W/cm^2)	3.8
Temperature (K)	868

These resulting graphs are similar in both the shape as well as pattern to the previous results. While the maximums are different they occur in the same manner and looking at the deceleration profile it is similar to the nominal case, where the peak deceleration happens upon detaching from the primary spacecraft. In this case the peak deceleration is 13 g's and occurs after peak heating takes place. In fact it is clear to see in Fig. 21 that the heating actually drops faster once the separation occurs.

Understanding how speed and angle of the entry changes the environment for the secondary payload is only part of what is necessary to understand the full problem. Another facet of the problem is the payload mass. By varying the mass of the secondary payload, the resulting maximums show how the mass of the payload affects the entire system. Figure 22 shows the results of varying the payload mass from 50 kg to 500 kg using a nominal entry trajectory of 7.6° and 5.5 km/s. Clearly, there is a trend where, as the mass increases, the acceleration decreases, however, at the same time the acceleration is dropping, the heat flux and temperature are rising. This means a spacecraft with more mass will have more heating concerns as a lighter spacecraft with the same ballute. This just brings the focus to what sort of design challenges a mission would undergo. It

would be necessary to carefully balance the ballute size and mass with the mass of the spacecraft so that an acceptable level of both heating and acceleration is achieved.

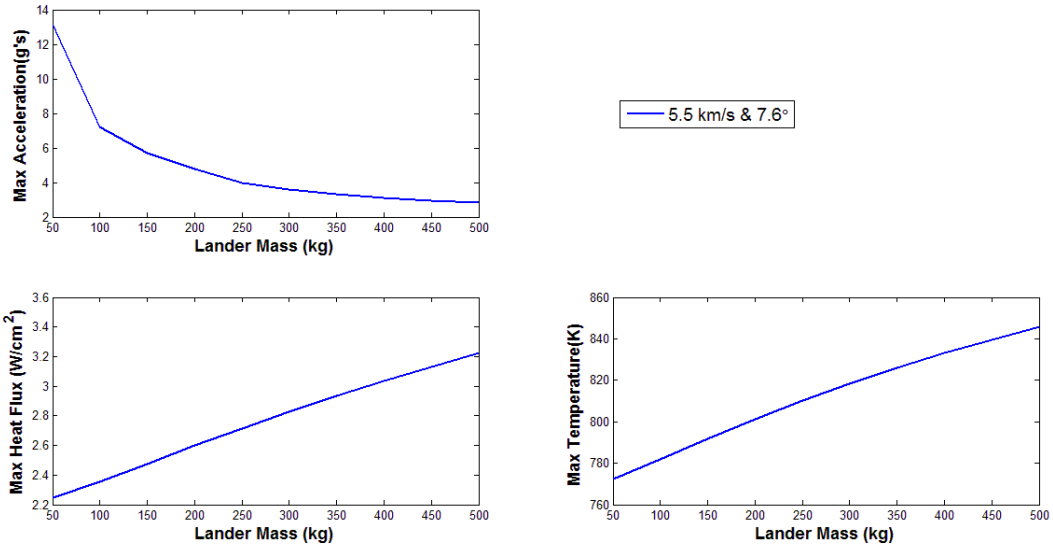

Figure 22. Maximum acceleration, heat flux, and temperature due to varying the secondary payload mass from 50 kg to 500 kg

5.3 Results Discussion

The maximum values of acceleration, heat flux, and temperature do not hold much meaning until they are compared with the maximum allowed values. These values are based on the assumption that the thin film material used for the ballute would be a current material such as Kapton. This sets the heat flux limit at 3 W/cm^2, and with a max heat flux of 2.9 W/cm^2 these trajectories are within the limit, although barely. However, using the extreme entry angle and velocity raises the maximum heat flux above the 3 W/cm^2 limit. At a heat flux of 3.8 W/cm^2 the mission is not possible with the current material choice. Using Kapton limits the entry angle and entry velocity to 8.2° and 6 km/s. The results clearly show that

the higher velocity and high angle entry trajectories cause higher deceleration forces and higher temperatures. While it is more desirable to keep the deceleration as low as possible, a robust design would allow for a deceleration of 13 g's. However, the heat flux is more problematic. With a heat flux limit due to the materials available, this means that in some instances the heat flux needs to be lowered, and there are several ways to do so.

One option to raise the heat flux limit is finding a different thin film material that can withstand a higher heat flux. While there is not anything currently available, with the design and testing of inflatable heat shields currently under way it is possible that such materials may need to be developed for those projects, which would then allow ballutes to be made with those materials and survive in more demanding environments [16,17,18,19,20].

If it is not possible to use other materials with a higher allowable heat flux, there is a way to slightly adjust how much heat flux is encountered. This could be accomplished by increasing the radius of curvature of the ballute, the minor diameter. This spreads out the heat load from the stagnation point, allowing for higher energy entry trajectories. Using the nominal trajectory at Mars, Fig. 23 shows how the heat flux and temperature are related to the radius of curvature. The curve of the graph shows how the larger radii have lower heat flux and thus a lower peak temperature. At a radius of one meter the heat flux is at 5 W/cm^2 and increasing the radius to 5 meters results in a heat flux of 2.2 W/cm^2.

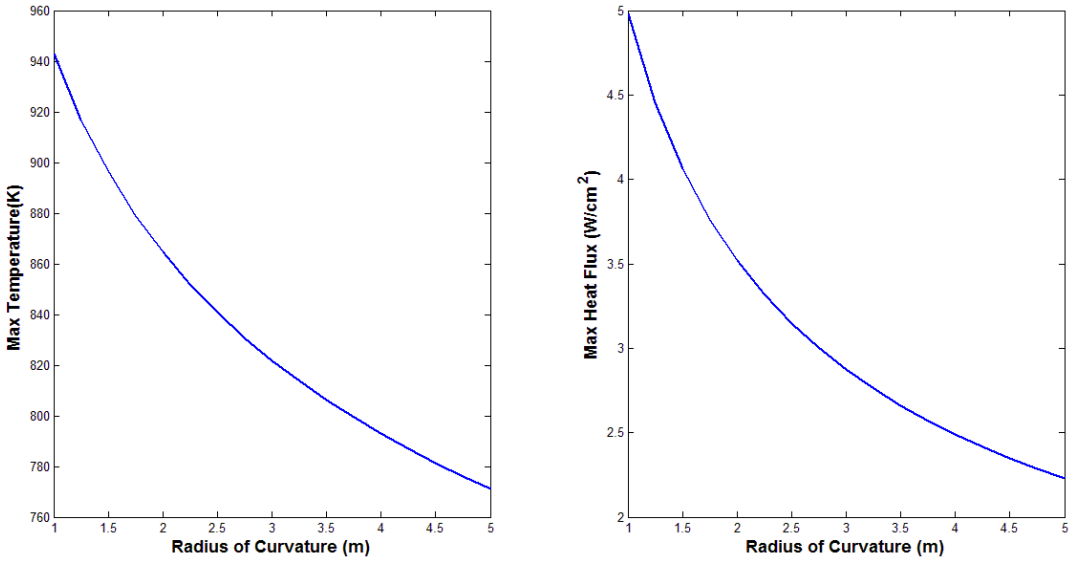

Figure 23. Radius of curvature versus heat flux and temperature

It is important to remember, however, that changing the radius does change the structural properties of the ballute. Since the effective area of the ballute is chosen to reach certain orbits through drag, the larger radii would result in a smaller toroid that could end up in the turbulent wake of the primary spacecraft. In the other direction, a radius that is too small could produce a ballute that would be prone to buckling. This can be done with a simple brute force optimization that ensures the stability and structural integrity of the ballute while keeping the heat flux low.

It is important to note that the peak deceleration of the secondary payload is different than what the primary spacecraft endures. The peak deceleration of the secondary payload happens during the separation from the primary spacecraft. So while the primary spacecraft would not encounter more than 4 g's from this particular design, the secondary payload would have a significant rise in the deceleration forces. This deceleration pattern is comparable to what would be

seen from a supersonic parachute slowing down its payload, and since the ballute is doing the job of a parachute this deceleration should be expected. After separation, the large area works on a relatively small payload to create the sudden spike in g-loading. Since the area of the ballute is fixed, due to its primary mission, there is not much that can be done to alleviate this force other than to use low velocity and shallow angle trajectories. For the most part, however, the payload will merely have to be able to handle the g-loading from separation. For reference, Mars Science Laboratory saw a g-force of about 9 g's from its parachute deployment and the Mars Phoenix Lander saw about 8.5 g's [14, 15]. While the method of entry and landing for both of those missions is not comparable to what is being studied here it does show what an acceptable g-load is at Mars.

Figure 22 shows that by varying the payload mass the acceleration dropped while the heat flux and temperature rose, which is important since this follows the trend normally seen on entry. Another important point is that the varying mass was done without changing the ballute design and on a nominal trajectory. Even though it seems that the payload mass could go up to about 350 kg before passing the 3 W/cm^2 limit for current materials, this does not take into consideration the extreme trajectory cases. As it has been shown, the extreme cases would need to have a design change for them to work, and the same principal is true here. A heavier secondary payload at the upper extremes would pass the 3 W/cm^2 threshold. This means that if a heavier payload is desired, a new design or a new material would need to be used.

Comparing the pre- and post-separation values helps us to understand how the design will need to be changed in order to survive entry. As Fig. 18 shows the maximum temperature is reached before the maximum deceleration. This is due to how the separation causes a spike in the deceleration force. Therefore the secondary payload would have a different g-force threshold compared to the primary spacecraft. However, the temperature maximum is the same for both. One difference in favor of a secondary payload is that separation happens after the maximum temperature is reached and then drops off rapidly. This means that the payload would not need much heat shielding compared to the spacecraft.

For the secondary payload to safely make it to the surface some sort of heat shield will have to be used. Sizing the heat shield will depend on the design of the payload itself. Due to the relatively low heat flux that the payload will encounter, a simple metal plate would suffice as the heat shield, especially since the time spent in the high heat flux environment post separation is of such a short interval. From the results shown the ballute can survive the entry into the atmosphere as long as the ballute material can withstand the heat and the ballute is designed to be structurally sound.

6. Entry at Other Destinations

6.1 Initial Values

The study at Mars shows the plausibility of using the ballute to land a mission on the planet as well as showing the accuracy of the simulation. The next step is to run the simulation on other possible missions to see if the ballute could be used for secondary missions at other planets. Since there have been proposed missions to both Titan and Venus these are good candidates for study.

The Titan Explorer mission that Miller proposes would put a satellite in orbit around the moon Titan [9]. This mission uses the initial values shown in table 13. Using the mission as a base, the system could be simulated to see if a secondary mission could be done utilizing the ballute. Compared to Mars, the entry angle is much steeper at 33.5-36.0° while at Mars it was 7.1-8.2°. The entry velocity is also higher at 9.6 km/s compared to the velocity at mars of 6 km/s. With a denser atmosphere this could cause some difficulties in both the heating and deceleration by causing them to go over the assumed limits.

Table 13. Initial values for the Titan Explorer mission [11]

Entry Angle (deg)	33.5-36.0
Entry Velocity (km/s)	9.6
Mass Spacecraft (kg)	325
Mass Lander+Ballute (kg)	68
Drag Coefficient, C_D	1.39
Entry Altitude (km)	1200
Ballutes cross-sectional area (m^2)	450
Spacecrafts cross-sectional area (m^2)	3
Emissivity (ε)	.9

.

For the mission to Venus a proposed sample return mission was used to study the usefulness of a ballute aerocapture[11]. Table 14 shows the initial values for the Venus mission which was based off of the mission studied by Hall *et al*. [7]. With an entry velocity of 11.6 km/s, the Venus mission has the highest entry velocity. However, the entry angle is 7.4-7.7° which is similar to the Mars mission. Due to the fact that the proposed mission is to return a sample from the planet's surface, the mass and the ballute area for the spacecraft is much higher at a total 3285 kg and 5031 m^2 respectively. Much like Titan, Venus has an atmosphere that is thicker than the one on Mars which will affect the heat and the deceleration.

Table 14. Initial values for the Venus sample return mission [7]

Entry Angle (deg)	7.4-7.7
Entry Velocity (km/s)	11.6
Mass Spacecraft (kg)	2600
Mass Lander+Ballute (kg)	685
Drag Coefficient, C_D	1.31
Entry Altitude (km)	200
Ballutes cross-sectional area (m^2)	5027
Spacecrafts cross-sectional area (m^2)	4
Emissivity (ε)	.9

6.2 Entry at Titan

In order to understand how a secondary mission would work at Titan the initial values from Table 13 were used in the simulation. To ensure that the results would be of the extreme case, the maximum values for the entry angle were used. The results of simulation are graphed in Fig. 24. By examining the graph, the separation point can be found 175 seconds after entry begins. This is characterized by either a spike or drop on the respective graph.

From the graph, the maximum deceleration can be seen to peak at 4 g's right at the time of separation. The maximum heat flux is 7.68 W/cm^2, which corresponds to a temperature of 1043 K. These values occur at about 125

seconds, which is before separation occurs. Since the heat flux is above the 3 W/cm^2 limit, the current material choice of Kapton would not be viable. However, since this heating peak occurs before separation that would mean for the mission itself to work a new material would have to be chosen anyway.

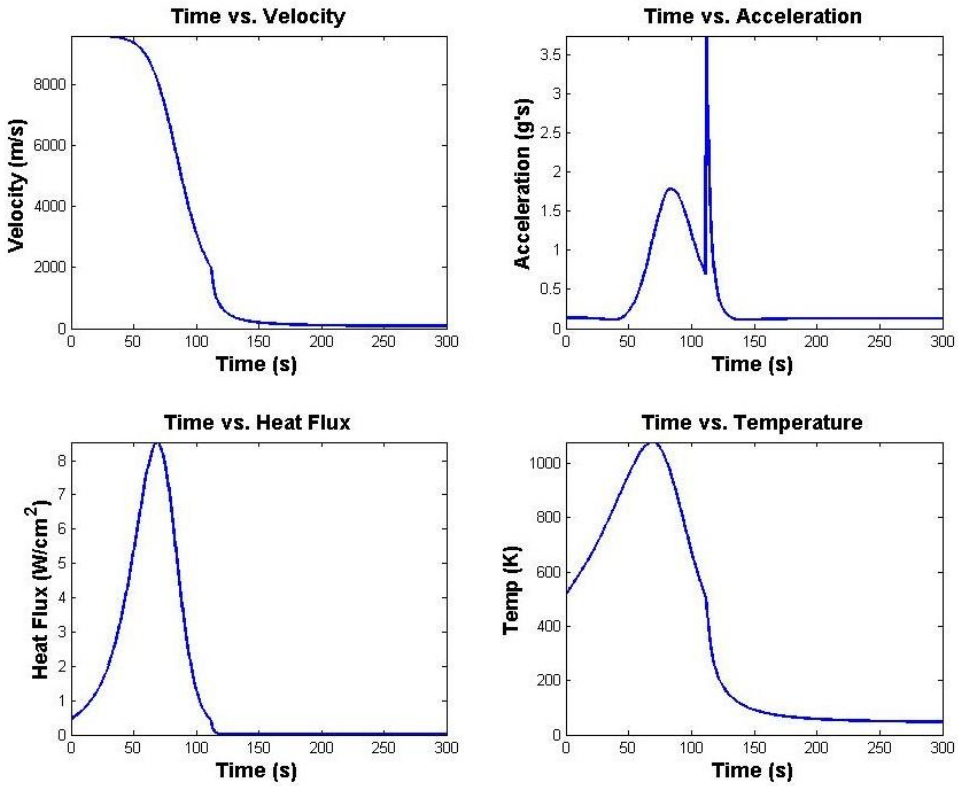

Figure 24. Velocity, acceleration, heat flux, and temperature vs. time for entry at Titan

6.3 Entry at Venus

Similar to the model done for Titan, the Venus entry used the maximum entry angle from Table 14 to ensure the most extreme response. The results of the simulation are graphed in Fig. 25. From the graphs the separation can be seen to occur at 42 seconds and the maximum heat flux is 6.2 W/cm^2 with a temperature of 990 K. Like the results for the Venus mission, the maximum heating at Titan

occurs before separation. However, in this case separation does occur much sooner after the peak. One major difference from the previous simulations is the maximum acceleration, which is 25.5 g's.

This g-load is high compared to the other missions, but it is not an insurmountable limit. Pioneer Venus faced deceleration closer to 300 g's [14]. With such a high entry velocity massive deceleration forces should be expected.

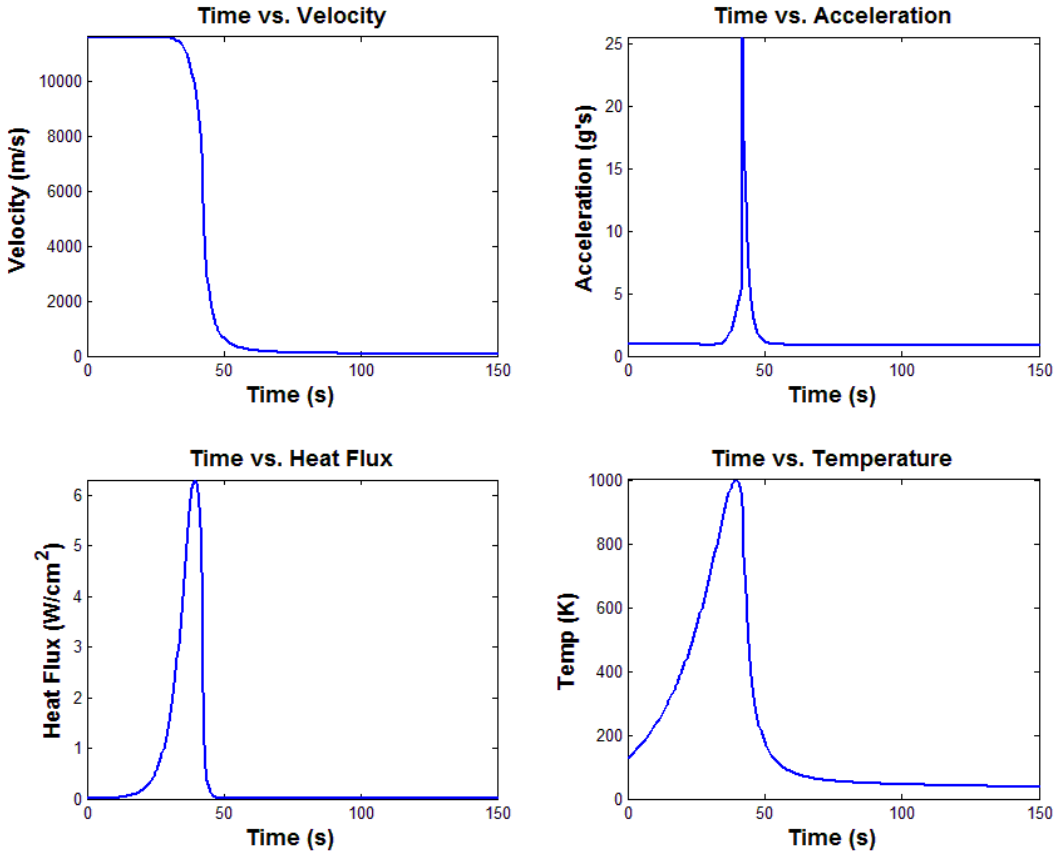

Figure 25. Velocity, acceleration, heat flux, and temperature vs. time for entry at Venus

6.4 Summary

Simulating the entries at both Titan and Venus depict some interesting results. First, at both Titan and Venus the heat flux is above 3 W/cm^2 at 7.68 and 6.20 W/cm^2 respectively. Such a high heat flux is a problem for the current material choice. As for the deceleration, at Titan the maximum deceleration according to the mission parameters is 4 g's, while at Venus the maximum is 25 g's. Both of these are acceptable values for the missions.

However, the most interesting result is related to the timing of the ballute separation. In all of the cases, whether it was at Mars, Titan, or Venus, the separation of the ballute would happen after the peak heating occurred. During separation is where the peak g-loading would occur, and yet it was usually during the peak g-loads for the normal aerocapture entry that separation would take place. This should not be surprising since separation depends on slowing down to a certain velocity and the graph clearly shows that it is during that deceleration that separation happens.

This is the most important result because it shows that as long as the ballute can survive the initial heating required for the primary aerocapture mission, it will be able to withstand the heating for the secondary entry. This means that a ballute optimized for the primary aerocapture mission can be re-tasked for a secondary mission with little to no impact upon the primary mission. The majority of the impact will come from the integration of the secondary spacecraft and the increased g-load that spacecraft will have to undergo.

7. Buoyancy

7.1 Buoyancy at Mars

Buoyancy could be a major issue. Depending on what the mission calls for and how the planet's atmosphere affects the ballute, the ballute could end up never actually landing. This becomes less of a concern if the mission does not need the ballute to actually reach the surface. If the ballute floats in the atmosphere, a weather station could be hung from it or a drone could be launched from it. Unfortunately, as Fig. 19 shows, the ballute does not float in the Martian atmosphere and goes directly to the ground. The reason for this is the fact that the Martian atmosphere is not very dense and thus is not conducive to buoyancy.

To see how buoyancy is affected by the volume of the ballute, a simulation was run varying the ballute's volume and finding the resulting minimum altitude at which the ballute will float, Fig. 26. The graph shows that not until the volume goes above 4000 m^3 does the ballute begin to float. The altitude gain is linear until it reaches the maximum volume of 10,000 m^3, which has the ballute floating at just over 5 km off the surface. Obviously, this shows that the ballute could be used to float a payload if that is what the mission requires. However, this would require a very large ballute and may not be the most efficient option due to sizing and weight concerns which might not be realistic for a Mars mission. A floating ballute could be viable on other planets, as long as the planet has a higher atmospheric density than Mars.

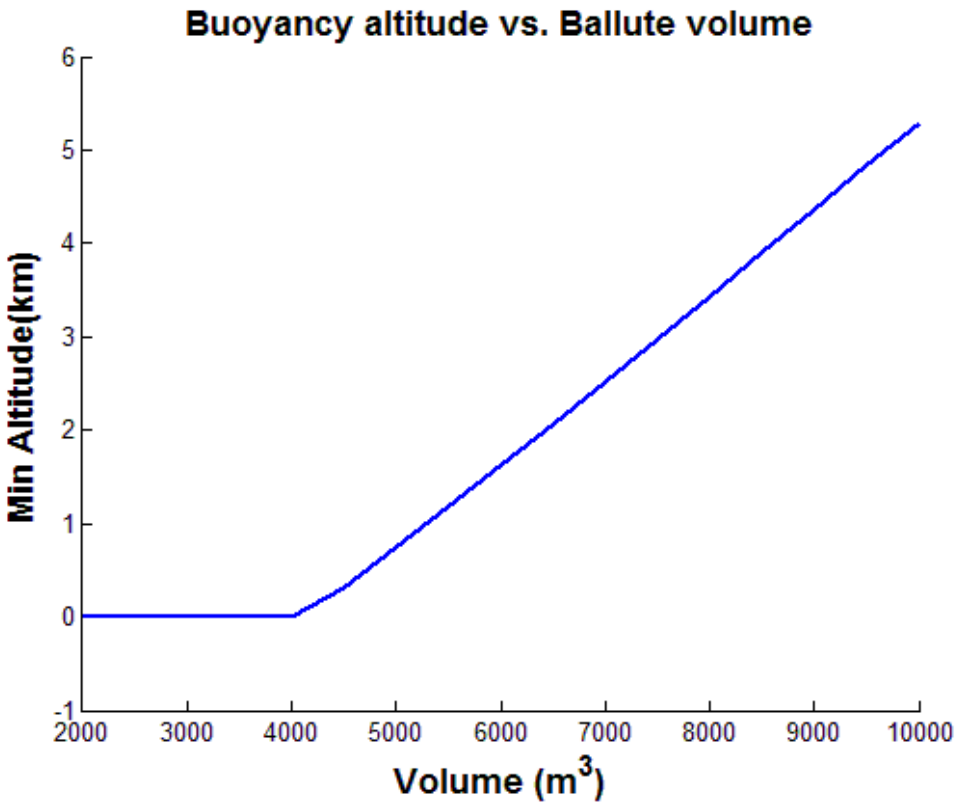

Figure 26. Minimum altitude due to buoyancy based on the ballute volume

7.2 Buoyancy at Venus

The buoyancy at Venus was also simulated to understand the response of the ballute after entry. Since Venus has a much thicker atmosphere the response should be drastically different. Again the initial values from the Venus mission were used in the simulation, Table 14. Only this time the volume of the ballute was set as a range from 1,000 to 100,000 m^3. Then, from the simulation, the final altitude was found. Figure 27 shows the final altitude based on the ballutes volume.

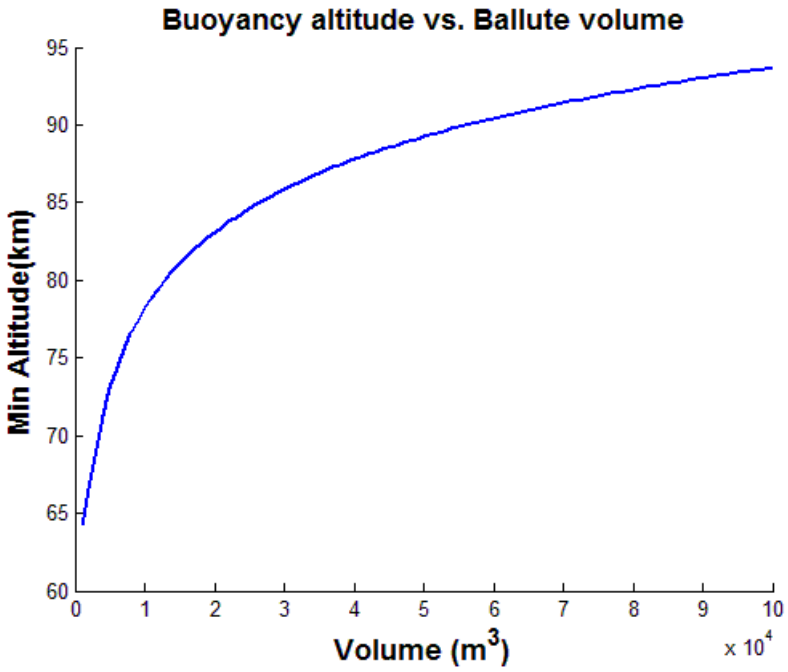

Figure 27. Ballute volume vs. minimum altitude at Venus

The figure shows how the ballute floats at 64 km when the volume is at 1,000 cubic meters. At 100,000 cubic meters the ballute floats at 94 km above the ground. Unlike the linear progression at Mars, Venus has more of a logarithmic growth. Because of the higher density atmosphere compared to Mars the buoyancy is much greater.

7.3 Buoyancy at Titan

Titan is another possibility for Ballute missions and so the buoyancy must be shown as well. The initial values of the mission are detailed in Table 13. For the volume the range was from 100 to 10,000 m^3. Figure 28 shows the ballute volume versus the final altitude.

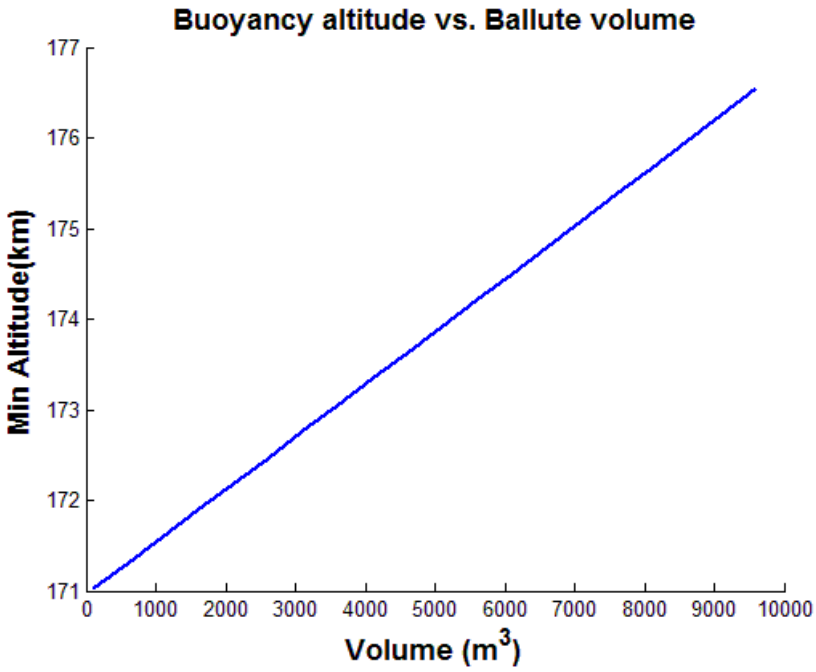

Figure 28. Ballute volume vs. minimum altitude at Titan

Once again, the denser atmosphere allows the ballute to float above the ground. With a minimum altitude of 171 km for a volume of 100 m^3 and an altitude of 176.5 km for a volume of 10,000 m^3 the progression happens linearly. However the differential is very small with a 100 times larger volume the difference in altitude is only 5.5 km.

7.4 Buoyancy Summary

The results show that buoyancy will be a factor in ballute missions. The extent to which it will affect the mission depends upon how large the ballute is and the atmospheric density of the planet. A high density will result in the ballute floating at a higher altitude, while with the low density found on Mars the volume needed to keep the ballute in the air becomes very high. Depending on the mission, it

may be useful to have the ballute floating at some altitude in the atmosphere to launch a drone or to take atmospheric measurements.

Whether or not it is easy to get the ballute at a desired altitude would depend on which planet the mission was going to and which altitude is desired. At Mars the atmosphere is not very thick and therefore it would take a large ballute to get it off the ground. Venus is more buoyant, however, it would still take a large ballute to raise the altitude above 65 km. In comparison, Titan has a range going from 171 to 176.5 km in altitude. In the end, while it is possible for the ballute to float in the atmosphere, the decision of whether or not the ballute should would have depend on the proposed mission.

8. Conclusion

Simulating the entry of a ballute and the second payload shows the viability of this design. The stability of the spacecraft during entry is due to the cg location and will be stable as long as the second payload meets the weight requirement. At Mars the ballute will undergo heating lower than the 3 W/cm^2 limit in place for current materials, as long as the appropriate trajectories are used. However, both the Titan and Venus entries show heating requirements closer to 7 W/cm^2 going beyond the limits of the current materials. While there is a large g-loading at separation due to the changed ballistic coefficient, it is similar to what is seen by other landers during entry and descent and would not impede the mission.

While buoyancy does prove to be a factor in the descent of the secondary payload at both Titan and Venus, it is not as much of a factor in the comparatively thin atmosphere of Mars. Although it is possible that a ballute's volume would be large enough to cause it to float above the Martian surface, it does not in this scenario. To have it do so would require much more volume and material. Thus it can be concluded that a successful aerocapture mission can be accompanied by an equally successful secondary use landed mission.

8.1 Future Work

For this work there are a few ways to improve the simulation. One change would be to import more planets for the code to simulate. This would allow a proposed mission to be evaluated for whether an aerocapture maneuver is possible, and also how a secondary payload would react. Another upgrade would be to implement a system that could provide the size and dimensions of the

ballute based off of the mission parameters and the desired limits for both the primary spacecraft and the secondary payload. A slightly more difficult upgrade would be to change the code so it can simulate six degrees of freedom. This would allow for a better understanding of the dynamics the spacecraft.

Overall there is still much work to be done before ballute aerocapture is a viable technology. Materials need to be tested for heat resistance and durability so that it will not only survive the heat of the maneuver, but also the packing, deployment, and the stress from the maneuver. With NASA developing a Hypersonic Inflatable Aerodynamic Decelerators (HIAD) [16, 17,18,19,20] these issues will be studied and it is likely that several of them could possibly be solved. The optimum design for the ballute must be finalized, the shape and orientation of the ballute determines how much heat and acceleration the system will see. Another important feature that has yet to be decided is how the ballute is attached to the spacecraft.

Designing the attachments includes both the number and material of the cables or even deciding if cables are the best way to attach the ballute to the spacecraft. Possibly a net style attachment would be better and would more easily distribute the loads. Finite element analysis will have to be done to understand the stresses put on the material and what is the best way to attach the ballute to the spacecraft.

The buoyancy of the ballute would have to be studied carefully depending on what planet the mission would be going to. If a specific altitude is required then a study should be done as to whether or not the ballute would be the best way to

attain and maintain the altitude. Adding a larger volume would impact the overall weight of the spacecraft. Also the larger volume would make the deployment and packing of the ballute more difficult.

Works Cited

[1] Brown, G. and Richardson, R., “Minimum-Mass Design for Titan Aerocapture,” AIAA Paper 2005-1637

[2] Reuben R. Rohrschneider and Robert D. Braun. "Survey of Ballute Technology for Aerocapture", Journal of Spacecraft and Rockets, Vol. 44, No. 1 (2007), pp. 10-23. doi: 10.2514/1.19288

[3] Nebiker, F. R., *et al*. PEPP Ballute Design and Development Final Report. Goodyear Aerospace Corporation, 1967, PEPP Ballute Design and Development Final Report.
https://ntrs.nasa.gov/archive/nasa/casi.ntrs.nasa.gov/19680010845.pdf

[4] Hacker, Barton C, and James M Grimwood. “On The Shoulders of Titans - Ch8-4.” NASA, NASA, www.hq.nasa.gov/office/pao/History/SP-4203/ch8-4.htm.

[5] Mayhue, Robert J, and Clinton V Eckstrom. “FLIGHT-TEST RESULTS FROM SUPERSONIC DEPLOYMENT OF AN 18-FOOT-DIAMETER (5.49-METER) TOWED BALLUTE DECELERATOR.” NASA Technical Reports Server, NASA Langley Research Center, ntrs.nasa.gov/archive/nasa/casi.ntrs.nasa.gov/19690017080.pdf.

[6] “MK82 Air Inflatable Retarder Bomb.” National Museum of the United States Air Force™, 29 May 2015, www.nationalmuseum.af.mil/Visit/Museum-Exhibits/Fact-Sheets/Display/Article/197591/mk82-air-inflatable-retarder-bomb/.

[7] Hall, J. L. and Le, A. K., “Aerocapture Trajectories for Spacecraft with Large, Towed Ballutes,” 11th Annual AAS/AIAA Space Flight Mechanics Meeting, Santa Barbara, CA, AAS 01-235, Feb. 11- 15, 2001.

[8] Masciarelli, Jim, and Kevin Miller. "Summary of Ultralightweight Ballute Technology Advances." NASA. Web.

[9] John Dec and Robert Braun. "An Approximate Ablative Thermal Protection System Sizing Tool for Entry System Design", 44th AIAA Aerospace Sciences Meeting and Exhibit, Aerospace Sciences Meetings, ().
http://dx.doi.org.ezproxy.lib.calpoly.edu/10.2514/6.2006-780

[10] Justus, C. G., and R. D. Braun. “Atmospheric Environments for Entry, Descent and Landing (EDL) .” 5 Nov. 2007, https://ntrs.nasa.gov/archive/nasa/casi.ntrs.nasa.gov/20070032693.pdf.

[11] Miller, K. L., Gulick, D., Lewis, J., Trochman, B., Stein, J., Lyons, D. T., and Wilmoth, R., “Trailing Ballute Aerocapture: Concept and Feasibility Assessment,” 39th AIAA/ASME/ASEE Joint Propulsion Conference and Exhibit, Huntsville, AL, AIAA Paper 2003-4655, July 20-23, 2003.

[12] Park, Chul, “Theory of Idealized Two-Dimensional Ballute in Newtonian Hypersonic Flow,” Journal of Spacecraft and Rockets, Vol. 25, No. 3, 1988, pp. 217–224;

[13] Daniel Lyons and Wyatt Johnson. "Ballute Aerocapture Trajectories at Neptune", AIAA Atmospheric Flight Mechanics Conference and Exhibit, Guidance, Navigation, and Control and Co-located Conferences, ().
http://dx.doi.org.ezproxy.lib.calpoly.edu/10.2514/6.2004-5181

[14] Chris Karlgaard, Prasad Kutty, Jeremy Shidner, Mark Schoenenberger, and Michelle Munk. "Mars Entry Atmospheric Data System Trajectory Reconstruction Algorithms and Flight Results", 51st AIAA Aerospace Sciences Meeting including the New Horizons Forum and Aerospace Exposition, Aerospace Sciences Meetings, ().
http://dx.doi.org/10.2514/6.2013-28

[15] Prasun Desai, Jill Prince, Eric Queen, Rob Grover, and Juan Cruz. "Entry, Descent, and Landing Performance of the Mars Phoenix Lander", AIAA/AAS

Astrodynamics Specialist Conference and Exhibit, Guidance, Navigation, and Control and Co-located Conferences, (). http://dx.doi.org.ezproxy.lib.calpoly.edu/10.2514/6.2008-7346

[16] Bienstock, B. J. Proceedings of the International Workshop Planetary Probe Atmospheric Entry and Descent Trajectory Analysis and Science, 6-9 October 2003, Lisbon, Portugal. Edited by A. Wilson. ESA SP-544, Noordwijk, Netherlands: ESA Publications Division, ISBN 92-9092-855-7, 2004, p. 37 - 45

[17] Levine, Jay. "Loads Tests Validate Design of Hypersonic Inflatable Aerodynamic Decelerator." NASA. Ed. Yvonne Gibbs. NASA, n.d. Web. 10 July 2016.

[18] Ellis, Sasha. "NASA Tests Inflatable Heat Shield Technology for Deep Space Missions." NASA. Ed. Samuel McDonald. NASA, 10 Mar. 2016. Web. 10 July 2016.

[19] Dunbar, Brian. “IRVE-3: Inflatable Heat Shield a Splashing Success.” NASA, NASA, 6 June 2013, www.nasa.gov/directorates/spacetech/game_changing_development/HIAD/irve3-success.html.

[20] Hall, Loura. “HIAD (Hypersonic Inflatable Aerodynamic Decelerator) Images.” NASA, NASA, 5 June 2014, www.nasa.gov/offices/oct/stp/game_changing_development/HIAD/images.html#lowerAccordion-set1-slide4.

[21] Medlock, K., Ayoubi, M., Longuski, J., & Lyons, D. *Analytic Solutions for Aerocapture, Descent, and Landing Trajectories for Dual-Use Ballute Systems. AIAA/AAS Astrodynamics Specialist Conference and Exhibit.* doi:10.2514/6.2006-6026

[22] Justh, Hilary L, et al. “Global Reference Atmospheric Models, Including Thermospheres, for Mars, Venus and Earth.” NASA Technical Reports Server, 1 Jan. 2006, ntrs.nasa.gov/archive/nasa/casi.ntrs.nasa.gov/20060048492.pdf.